



Design and Fabrication of a Solar PCM Heat Exchanger for Indoor Temperature Stabilization

Project Supervisor: Dr. Abdur Rehman Mazhar

Group Members:

Muhammad Shariz
Abdullah Nasir
Munam Ali
Haider Ali

DECLARATION

We hereby declare that work included in this document is not copied from any other source published or submitted in any educational institute. In case of any plagiarism found, we take full responsibility for any disciplinary action taken against us.

Signatures:

Dr. Abdur Rehman Mazhar

Muhammad Shariz

Abdullah Nasir

Munam Ali

Haider Ali

COPYRIGHT STATEMENT

- The student author retains the copyright in the text of this thesis. Only in compliance with the author's instructions and registered in the Library of NUST College of EME, copies (by any method) in full or excerpts may be created. The Librarian can provide further information. This page must be included in all copies created. Without the author's consent (in writing), more copies in compliance with such instructions may not be created.
- Subject to any prior agreement to the contrary, ownership of any intellectual property rights described in this thesis is vested in NUST College of EME and may not be made available for use by third parties without the written permission of the College of EME, which will prescribe the terms and conditions of any such agreement.
- The Library of NUST College of EME, Rawalpindi, has more information on the situations under which disclosures and exploitation may occur.

ACKNOWLEDGEMENTS

We are grateful to Allah Almighty, the Most Merciful, and Al Fattah for the blessings, courage, and intelligence He has bestowed upon us, which has enabled us to achieve such a magnificent objective.

We are grateful to our parents and family for their unwavering support and encouragement in the face of adversity. We owe a debt of gratitude to our supervisor, Dr. Abdur Rehman Mazhar for his constant advice and the time he spent supporting and encouraging us at each level. We would not have been able to do so much without his efforts. Furthermore, we are thankful to all of our colleagues and friends who have provided us with intellectual and emotional support.

ABSTRACT

The mismatch between energy demand and supply has provoked the researchers to look for clean and alternate energy supply methods. Thermal storages are cheaper and have high density whereas solar energy is renewable. Therefore, Solar systems incorporated with phase change materials (PCMs) as a thermal storage have significant plausibility to serve in this context. These systems are not yet able to endure the energy demands significantly but are being constantly improve. The aim of this project is to design and fabricate a Solar System integrated with a PCM thermal storage heat exchanger for achieving comfortable room temperatures in winters with almost zero operating cost. This project includes a review paper on Solar PCM Systems, a conference paper, submitted and to be presented in 19th International Bhurban Conference on Applied Sciences and Technology (IBCAST), a solar PCM heat exchanger designed for a small-scaled room and a research paper based on the testing of the fabricated system. The review paper will be focused on architectures of Solar systems integrated with PCMs tested by numerous researchers. Based on the extensive research on pre-existing Solar PCM systems, a novel design approach of Solar PCM System will be devised for indoor heating in winter conditions of Pakistan. A model based on this novel design is fabricated and installed. The fabricated model is tested in winter conditions and a research paper studying the room temperature and certain other associated parameters will be written. A parametric study is also conducted using an experimentally validated Computational Fluid Dynamics analysis.

NOMENCLATURE & ABBREVIATIONS

Nomenclature	
Q	Energy/heat, J
T	Temperature, T
m	Mass, kg
V	Volume, m ³
H	Enthalpy
S	Location of phase change interface
A	Area, m ²
h	Convection coefficient, W/m ² .K
Q̇	Heat flux, W/s
h_{fg}	Latent heat of fusion, kJ/k
Q_{conv}	Heat transfer due to convection
Q_r	Heat transfer due to radiation
D	Half thickness of the fin
k	Ratio of heat conductivities
Dimensionless number	
Nu	Nusselt number
Ri	Richardson number
Greek letters	
τ	Time, s
ε	Rate of solidified PCM
λ	Root of the transcendental equation
□	Dimensionless temperature distribution
ζ	Modified Stefan Number
Abbreviations	
PCM	Phase change material
SPCMS	Solar phase change material systems
TES	Thermal energy storage
LHS	Latent heat storage
HVAC	Heating, ventilation, and air-conditioning
PTTS	Passive thermal storage system
ATTS	Active thermal storage system
UHI	Urban heating island
DWH	Domestic water heating
DP-SAH	Double pass solar air heater
GW	Gray water
TPF	Thermal performance factor
FEM	Finite element method
FVM	Finite volume method
FDM	Finite difference method

Table of Contents

DECLARATION	2
COPYRIGHT STATEMENT	3
ACKNOWLEDGEMENTS	4
ABSTRACT	5
NOMENCLATURE & ABBREVIATIONS	6
Chapter 1: Introduction	12
1.1 <i>Background</i>	12
1.2 <i>Objective</i>	12
1.3 <i>Thermal Energy Storage</i>	13
1.3.1 Significance of Thermal Storage	13
1.3.2 Types of Thermal Energy Storage	14
1.4 <i>Energy Storage System</i>	15
1.5 <i>Classification of PCM</i>	15
1.6 <i>Scope</i>	16
1.7 <i>Motivation</i>	16
Chapter 2: Literature Review	16
2.1 <i>Thermophysical Properties of PCM</i>	19
2.2 <i>Key Performance Indicators</i>	22
2.2.1 Thermal Performance Indicators	22
2.2.2 Economic Indicators	23
2.3 <i>Solar Integrated PCM Systems</i>	25
2.3.1 Active Systems	26
2.3.2 Passive Systems	34
2.4 <i>Solar PCM Optimization Techniques</i>	37
2.4.1 Theoretical Optimization	37
2.4.2 Numerical based Optimization	40
Chapter 3: Design and Calculation of PCM Heat Exchanger	42
3.1 <i>Design Approach</i>	42
3.2 <i>Design Requirements</i>	43
3.3 <i>Material Selection</i>	44
3.3.1 PCM	44
3.3.2 Heat Exchanger	45
3.3.3 Control Room	45
3.4 <i>Room Design</i>	45
3.5 <i>Heat Exchanger Design</i>	45
3.6 <i>Calculations</i>	46

Chapter 4: CAD Modelling	49
4.1 Heat Exchanger Unit	50
4.1.1 Top Header	50
4.1.2 Tubes	51
4.1.3 Shell	51
4.1.4 Main Header	51
4.2 Heat Exchanger Assembly	52
Chapter 5: Fabrication and Component Procurement	52
5.1 Procurements	53
5.2 Fabrication of Single Heat Exchanger Unit	53
5.3 Assembly of Fabricated Heat Exchanger Units	54
5.4 Fabrication of Control Room	55
Chapter 6: CFD Validation	56
6.1 Two-Dimensional Simulation	56
6.1.1 Two-Dimensional Domain Creation	56
6.1.2 Meshing	57
6.1.3 Boundary Conditions and Initialization	57
6.1.4 Models Used	57
6.1.5 Calculation Activities	58
6.1.6 Contour Plots and Results	58
6.2 Three-Dimensional Simulation	59
6.2.1 Geometry Creation	59
6.2.2 Meshing	60
6.2.3 Boundary Conditions and Initialization	61
6.2.4 Models	61
6.2.5 Calculation Activities	61
6.2.6 Contour Plots and Results	62
Chapter 7: Experimentation	63
7.1 Actual Experiment	64
7.1.1 Installation	64
7.1.2 Auxiliary Components	65
7.1.3 Arduino Setup	67
7.2 Cautions	68
7.2.1 Leakage	68
7.2.2 Pump Tripping	68
7.2.3 Water Temperature	68
7.2.4 Sensor Reading	69
7.3 Results	69
7.3.1 Charging	69
7.3.2 Discharging	70
Chapter 8: Comparison of Results	70
Chapter 9: Discussion on Conventional Analysis Techniques	71

Chapter 10: Future Recommendations and Limitations	73
<i>10.1 Future Recommendations</i>	73
<i>10.2 Limitations</i>	74
10.2.1 Phase Change Material	74
10.2.2 System Designed	75
Chapter 11: Conclusion	75
REFERENCES	76

List of Figures

FIGURE 1: TYPES OF THERMAL ENERGY STORAGE	15
FIGURE 2: CLASSIFICATION OF PCM	16
FIGURE 3: FLOW DIAGRAM OF SPCMS	26
FIGURE 4: SCHEMATIC OF SOLAR INTEGRATED PCM SYSTEMS	26
FIGURE 5: PCM EMBEDDED IN A WALL	38
FIGURE 6: ICCSSW WITH AND WITHOUT PCM	40
FIGURE 7: DIFFERENT CONFIGURATIONS OF PCM SLEEVE TUBES (A) WITHOUT FIN ; (B) HALF FINS ; (C) FULL FINS	41
FIGURE 8: HEAT EXCHANGER DESIGN	42
FIGURE 9: FLOW DIAGRAM OF DESIGN APPROACH	43
FIGURE 10: UNIT EXCHANGER	46
FIGURE 11: SINGLE EXCHANGER UNIT	50
FIGURE 12: TOP HEADER	50
FIGURE 13: A TUBE	51
FIGURE 14: SHELL	51
FIGURE 15: BOTTOM HEADER	51
FIGURE 16: MOUNTING FRAME	52
FIGURE 17: HEAT EXCHANGER	52
FIGURE 18: SINGLE EXCHANGER UNIT WITHOUT SHEET COVERING	54
FIGURE 19: TOP AND FRONT VIEW OF ASSEMBLY	55
FIGURE 20: CONTROL ROOM	55
FIGURE 21: 2D GEOMETRY	56
FIGURE 22: STRUCTURAL MESH	57
FIGURE 23: INITIAL CONTOUR PLOT OF TEMPERATURE	58
FIGURE 24: FINAL TEMPERATURE CONTOUR PLOT	59
FIGURE 25: THREE-DIMENSIONAL SIMULATION GEOMETRY REPRESENTATION	60
FIGURE 26: OVERALL THREE-DIMENSIONAL REPRESENTATION	60
FIGURE 27: THREE-DIMENSIONAL MESH	61
FIGURE 28: VOLUME RENDER AT START OF THE SIMULATION	62
FIGURE 29: VOLUME RENDER AT THE END OF SIMULATION	63
FIGURE 30: EXPERIMENTAL SETUP	64
FIGURE 31: PUMP	65
FIGURE 32: THERMOSTAT	65
FIGURE 33: VERNIER SURFACE TEMPERATURE SENSOR	65
FIGURE 34: ARDUINO SETUP	67
FIGURE 35: CHARGING DATA GRAPH	69
FIGURE 36: DISCHARGING DATA GRAPH	70

List of Tables

TABLE 1: THERMOPHYSICAL INDICATORS	19
TABLE 2: ENERGY AND ECONOMIC SAVINGS IN DIFFERENT LITERATURES	25
TABLE 3: SUMMARY OF REVIEW PAPERS IN ACTIVE DOMAIN	26
TABLE 4: SUMMARY OF REVIEW PAPERS IN PASSIVE DOMAIN	34
TABLE 5: PROPERTIES OF PARAFFIN WAX	44
TABLE 6: ROOM DIMENSIONS	45
TABLE 7: ITERATIONS FOR MASS CALCULATION	47
TABLE 8: DIMENSIONS OF ONE UNIT OF HEAT EXCHANGER	47
TABLE 9: SPECIFICATIONS OF THE HEAT EXCHANGER	49
TABLE 10: TWO-DIMENSIONAL SIMULATION RESULTS	59
TABLE 11: RESULTS OF THREE-DIMENSIONAL SIMULATION	63
TABLE 12: VERNIER SURFACE TEMPERATURE SENSOR SPECIFICATIONS	66
TABLE 13: RESULTS COMPARISON	71
TABLE 14: ADAPTABILITY OF ANALYSIS TECHNIQUES OF PCM HEAT EXCHANGER TOWARDS PASSIVE HEATING	71

Chapter 1: Introduction

1.1 Background

The amount of greenhouse gas emitted by ozone is steadily growing. Not only that, but high fuel costs and overuse of one source of energy have either generated a scarcity of energy supplies or increased the cost of it. Major energy resources are being squandered owing to inefficient methods of maintaining and storing energy sources. All of these factors are driving forces in attempts to provide and effectively utilise renewable energy supplies. One approach is to create energy storage devices, which are just as vital as developing a new renewable energy source. The stored energy can be turned into whichever form is desired. The energy storage system is today's technological problem.

Solar energy is one of the most brilliant and widely available forms of energy on the planet. Scientists from all over the world are trying to figure out the most efficient way to use solar energy. Solar energy, on the other hand, is the most wasted energy on the planet.

Thermal energy is already being used, as is the conversion of thermal energy to electricity. The issue it raises is that power can only be generated as long as sunlight is available. This is when heat storage becomes necessary. Thermal energy storage can also be used during the hours when the sun is not shining. It would also increase the operation of a power production plant by balancing load, and improved efficiency would result in energy saving and lower generation costs, making solar energy a viable option.

The use of Phase Change Material is one of the potential strategies for thermal energy storage. The usage of a phase transition material-based latent heat storage device is an efficient technique to store solar thermal energy. It has a high energy storage density and a short heat transfer temperature interval. PCMs have been widely employed in heat pumps and spacecraft thermal control systems to store latent heat.

1.2 Objective

The goal of this project is to design and build a phase change material heat exchanger that can be utilised as a thermal energy storage device using shell and tube construction. This technique will be integrated with solar water heaters in the future, allowing the water heater to heat water during non-sunlight periods using a thermal storage system.

1.3 Thermal Energy Storage

Thermal energy storage (TES) is a technology that stocks thermal energy by heating or cooling a storage medium so that the stored energy can be used later for heating and cooling applications and power generation.

1.3.1 Significance of Thermal Storage

A significant amount of energy is consumed by buildings to provide thermal comfort for the inhabitants, and this contributes to serious climatic changes. Hence, there is an urgent need to reduce the thermal energy consumption by this residential sector. Scientists and researchers are working on reaching zero energy buildings and thermal energy storages (TES) seem the best way to reach this goal [1]. In today's world, the usefulness of thermal energy storage is well known, and it seems hopeful prospect towards achieving a low-carbon future. TES technology is described as an initiative towards reduction in energy consumption in buildings. It aims to lessen the urban heating island (UHI) effects in cities and increase the energy efficiency and thermal comfort by balancing the energy demand between day and night [2]. Energy can be stored either physically or chemically. Physically, energy is stored as sensible and latent energy while thermochemical energy is when a chemical reaction occurs with heat of reaction.

Sensible and latent heat storage are mostly considered for building applications, although thermochemical energy storage is growing in interest within researchers of today. In sensible heat TES, massive materials like concrete, stone etc. are used to store significant amount of thermal energy, on the other hand, in latent heat TES larger amount of energy per volume can be stored using phase transition of the storage material known as the phase change materials (PCM) [3]. Thermal energy although is a low-grade energy but is encountered in abundance. Geothermal and solar energy are the largest sources of thermal energy. Solar energy is renewable, clean, and very easy to harness. But its limitation of being available for limited hours in a day is the rational for thermal storages [4]. Thermal storages could be in form of sensible heat or latent heat. As it is well known that latent energy is large as compared to sensible energy and does not cause a temperature change during phase change. So, materials having flexible transition temperatures and high latent heat can serve as potential thermal storage candidates.

PCM's are characterized by high latent heat of fusions and various PCM's with various transition temperatures are readily available which makes them very good thermal storage. Moreover, PCMs are of low cost, have high storage density and operate isothermally [5]. Some good PCMs are paraffin waxes, salt hydrates, fatty acids, and sugar alcohols. The major disadvantage of using PCMs is their very low thermal conductivity. Salt hydrates and fatty acids have better thermal conductivity, but they are chemically active and undergo incongruent melting. Due to this reason Paraffin waxes despite their low thermal conductivity are preferred as a thermal storage medium due to their easy handling, low cost, availability, congruent melting, and chemical stability. Various studies and experiments have been done as stated earlier for enhancement of thermal conductivity of PCMs like inserting graphite particles, nano particles, honeycomb fillers, internal fins, and carbon fibers etc. [6]. The PCM-based thermal energy storage systems used in buildings are of two types: active and passive storage systems. Active systems involve auxiliary devices to help charge and discharge a storage tank. On the other hand, passive systems do not need such heat exchangers to extract heat or cold from the storage. The incorporation of PCM in building can be in two forms: PCMs in building components like wall, floor, ceiling etc and PCMs in heat and cold storages. The former are the passive systems while the latter are active systems [7].

1.3.2 Types of Thermal Energy Storage

These storage mediums are characterized by high latent heat of fusion. In a thermal storage, heat is absorbed or released when the material transforms from one phase to another. Due to this ability, these storages are classified as latent heat storage units. There are three types of phase changes: solid-liquid, solid-gas, liquid-gas phase change. Due to the involvement of large amount of volume change, the phase change from solid gas and liquid gas is eliminated, hence solid-liquid phase change is preferred Latent Heat Storage.

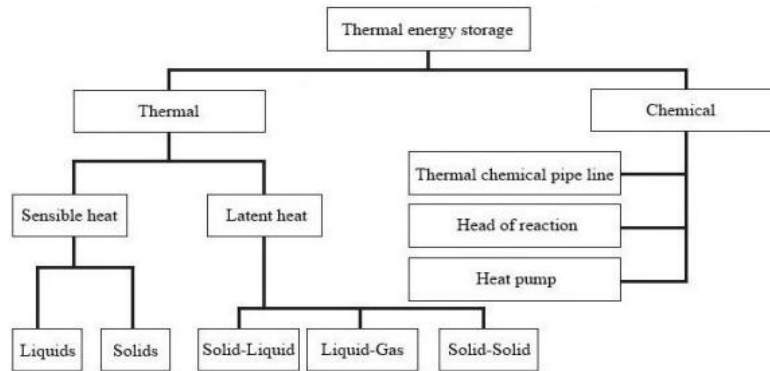


Figure 1: Types of thermal energy storage [8]

1.4 Energy Storage System

An energy storage system can be described in terms of the following characteristics:

Capacity: It defines the energy stored in the system and depends on the storage process, the medium, and the size of the system.

Power: It defines how fast the energy stored in the system can be discharged (and charged).

Efficiency: It is the ratio of the energy provided to the user to the energy needed to charge the storage system. It accounts for the energy loss during the storage period and the charging/discharging cycle.

Storage period: It defines how long the energy is stored and lasts hours to months (i.e., hours, days, weeks, and months for seasonal storage).

Charge and discharge time: It defines how much time is needed to charge/discharge the system.

Among the latent heat storages, PCM storages are widely used due to their easy of handling and cheaper cost.

1.5 Classification of PCM

PCMs can be classified into three categories: organic, inorganic and eutectics of inorganic and organic compounds, depending on the required temperature range. A detailed classification of PCM is shown in Figure 2.

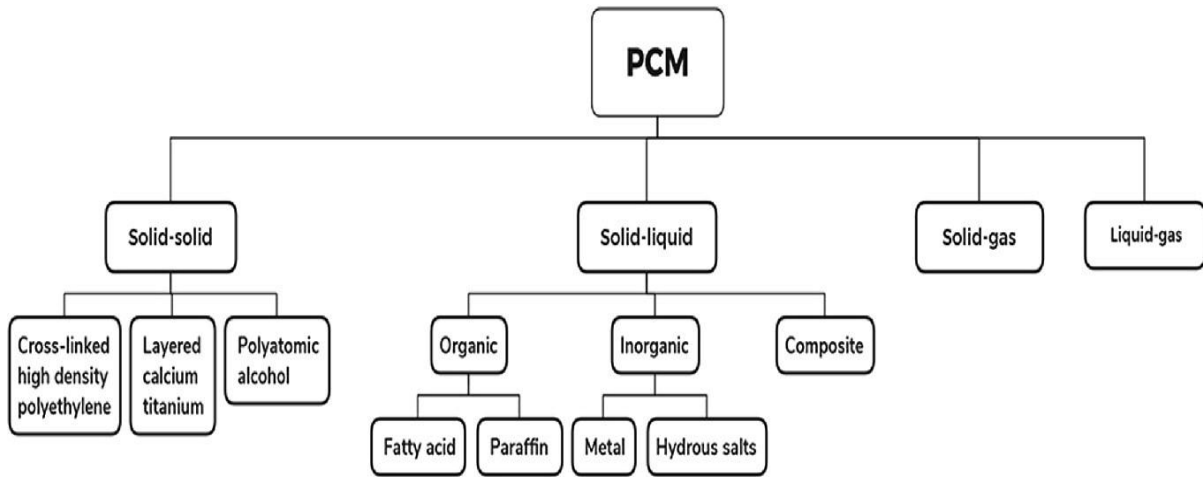


Figure 2: Classification of PCM [9]

1.6 Scope

An energy storage heat exchanger will be designed and built as part of the project. The storage substance is paraffin wax, which is utilised to store thermal energy efficiently. Paraffin wax will be included into the heat exchanger, allowing the system to function as a thermal energy storage device, storing solar thermal heat in paraffin wax and then using the thermal heat to heat water during non-sunlight periods.

1.7 Motivation

The tenets that led to the selection of this project are listed below:

- Devise a system capable of reducing the energy demands in both industrial and non-industrial sectors of Pakistan.
- Devise system with minimal operating cost
- Devise a system that provides clean energy
- Devise a system that efficiently harness renewable energy source.

Chapter 2: Literature Review

Energy consumption in the world is increasing exponentially. We stand in an era where natural energy resources are depleting at an expeditious rate and their demand is raising without bounds. In industrial countries one-third of the total energy is consumed by HVAC systems only [10]. This leads us to devise methods for providing alternative energy resources especially for heating and cooling requirements. Researchers have studied the use of

renewable energies to share the burden of energy consumption in buildings. Amongst all renewable energies, solar energy is vastly researched upon in conjunction to indoor environments because it is clean, easy to harness and safe [11]. Energy from the sun can be directly used to heat buildings or alternatively it can be concentrated on thermal collectors which in turn heat the carrying medium like water; that carries the heat through the system and supplies it to the desired area. The use of thermal collectors results in more absorption of solar energy as compared to direct heating and hence are preferred [12]. Due to the limited number of daily hours of sunlight, the working of solar systems is also limited. This problem can be addressed by integrating a thermal storage system with solar systems. Over the years latent heat storage (LHS) has been the focus of many researchers within the thermal energy storage domain [13].

The concept of LHS is to incorporate a material which changes phase during its operating temperature range and releases or absorbs large amount of latent energy which can be given to or extracted from the system in non-solar hours. PCMs are best for thermal storage due to their low cost, easy construction, high latent heat of fusions, flexible transition temperatures, high storage density, and isothermal operation. Several materials can serve as PCMs including paraffin waxes, salt hydrates, fatty acids, and sugar alcohols. Among all, paraffin waxes are widely used because they are cheap, readily available, and chemically stable [5]. The performance of PCMs is limited due to their low thermal conductivity and persistent efforts are being made to improve it. Researchers have used a graphite matrix, internal fins, honeycomb fillers and carbon fibres to enhance this thermal conductivity [14][15][16][17].

Over the years, incorporation of PCMs as thermal storage has been the focus of researchers. A. Khan et al [18] reviewed solar collector designs integrated with PCMs. Their review was primarily focused on different types of thermal collectors such as flat plate water collectors, flat plate air collectors, parabolic collectors, and evacuated tube collectors resulting in higher absorption of radiation. They also briefly explored different perspectives through which PCMs can be integrated with solar collectors. They found that large collector area, large PCM layer thickness, large flow rates result in better thermal performance of the system. They found evacuated tube collectors to provide higher outlet temperatures indicating the feasibility of using high transition temperature PCMs with them. Moreover, they found parabolic collectors to have the potential to replace the existing thermal collector technologies; if more radiation could be concentrated on them because they have lower

surface area which inhibits their thermal performance. M.E. Zayed et al [19] comprehensively reviewed cascaded PCMs to provide thermal storage for solar water collectors. Their review emphasized on the structure of solar collectors and cascaded PCM storages for water heating. They classified solar collectors based on tracking and degree of freedoms along with their essential components like frame, seals, insulations, absorber plates, tubes, glass covers etc. Their review revealed that PCMs compounded in descending order of their melting temperatures significantly increases thermal storage capacity and charging/discharging time. Such cascaded PCMs are more suitable for large scale applications where different grades of energies required. They concluded that myristic acid and paraffin wax with transition temperature ranging from 50°C to 60 °C are best for solar water heating systems. R.M. Muthusivagami et al [20] reviewed solar cookers with and without PCMs. They classified cookers as direct type, box type and concentrating type.

They concluded that box type solar cooker having a thermal storage are best for farmers for cooking their noon meal and it is installed in different parts of India. Moreover, their study revealed that parabolic concentrators provide high absorption of radiation, enough to generate steam and provide thermal energy for cooking at community level.

A review of SPCMS for drying of agricultural, seed grapes and food crops was done by Shalaby et al [21]. They assessed solar air heaters and exhaust air heaters for crop drying having PCMs directly and indirectly embedded in them. Their review revealed that appropriate flow rates with sufficient PCM embedded into the system can provide up to 68% energy savings. They found that lower thermal conductivity was the main hindrance in the thermal efficiency of these systems and therefore, they extensively reviewed the thermal conductivity enhancement techniques of PCMs. Chaturvedi et al [22] reviewed the applications of PCM in solar thermal storage. They classified thermal storages as sensible thermal storage, thermo-chemical storage, and latent heat storages. Latent heat storages were found to be very promising with materials that have high phase change energy (phase change materials) and high density. They broadly classified phase change materials as solid-solid, solid-liquid, solid-gas, and liquid-gas. Solid-solid phase change materials include cross-linked high-density polyethylene, layered calcium titanium and polyatomic alcohol. Solid-liquid PCMs include organic, inorganic, and composite PCMs. They reviewed applications of PCMs in buildings, water heating, photovoltaic heat management. They concluded that application of PCMs in photovoltaic heat management provides best results as it not only

improves electrical performance through cooling of photovoltaic panels but also provide useful thermal energy. Omara et al [23] reviewed the incorporation of PCMs for improving productivity of active and passive solar stills. They scrutinized numerous types of solar stills such as double slope solar stills, single stage solar stills, weir-type cascade solar stills, triangular pyramid solar still, tubular solar still, V-corrugated absorber solar still etc. Flat plate collectors, concentrators and heat pumps were also integrated into these systems for improving their thermal performance. In comparison with solar still without PCM, passive solar stills increased the productivity to 120% and active solar stills increased the productivity to 700% on inclusion of PCM.

We can infer from the preceding literature review that most of the work done in the domain of SPCMS is focused on either the solar collectors or PCM incorporation and not their integration. As of the field of application: water heating, crop drying, and photovoltaic heat management has been vastly researched.

We find comparatively less work on solar systems integrated with PCMs for domestic use. The scope of this project lies in the review, fabrication, and testing of novel architecture of a solar PCM system for indoor temperature and humidity stabilization.

2.1 Thermophysical Properties of PCM

After extensive research on novel architectures of solar PCM Systems, the focus of the researchers shifted towards optimization of these systems. This initiated a new paradigm towards efficient, low cost and clean energy systems. The idea was to study the performance of solar PCM Systems by varying various parameters such as the tube pitch, tube diameters, angle of solar collector, thermophysical properties of the used PCM etc.

Table 1 reviews such technical and thermophysical indicators of PMCs:

Table 1: Thermophysical Indicators

Indicator	Variation	Outcome	Ref.
Transition temperature of PCM	<ul style="list-style-type: none"> The transition temperature of PCM should be within the operating range of the system 	<ul style="list-style-type: none"> The latent heat is extracted and stored efficiently during the operation of the system 	[24]

Density of PCM	<ul style="list-style-type: none"> The density of PCM should be high 	<ul style="list-style-type: none"> This will reduce the volume of the thermal storage so that more energy can be stored in less volume 	[24]
Latent heat of fusion of PCM	<ul style="list-style-type: none"> Latent heat of Fusion of PCM should be high 	<ul style="list-style-type: none"> This will result in high density and consequently more energy 	[25]
Specific heat of PCM	<ul style="list-style-type: none"> Specific heat of PCM should be high 	<ul style="list-style-type: none"> This corresponds to high density energy storage which is desirable 	[24]
Thermal conductivity	<ul style="list-style-type: none"> The main concern regarding PCM thermal storage is their lower thermal conductivity. The use of graphite powder, carbon nanotube, graphene, Honeycomb filler, Aluminium Matrices, carbon fibres and nanoparticles in PCM. 	<ul style="list-style-type: none"> These will help in increasing the thermal conductivity of PCM 	[26]
Tube-Tube distance in PCM heat exchanger	<ul style="list-style-type: none"> The distance between tubes of heat exchangers plays significant role in its performance The distance between the tubes should be decreased in order to make the system compact. 	<ul style="list-style-type: none"> This reduces the loss of heat to the surrounding It generates the space for more tubes causing an increase in heat transfer area 	[27]
Insulation of solar PCM system	<ul style="list-style-type: none"> Transfer of energy from solar absorber to the heat carrying medium has a great negative effect on performance of the system Insulation on the heat carrying medium tube walls should be 	<ul style="list-style-type: none"> Preventing such heat loss can increase the performance of the system significantly 	[28]

	done. Mostly Polyurethane and Wood are used for insulation.		
Circulation flow rate	<ul style="list-style-type: none"> The useful heat gain is found to be increased with the increase in flow rate of the circulating fluid. Thus, the flow rate should be increased. 	<ul style="list-style-type: none"> This will consequently cause an increase in heat transfer to the facility for which the system is employed 	[29]
Cascaded PCM arrangement	<ul style="list-style-type: none"> Using two PCMs having different transition temperatures 	<ul style="list-style-type: none"> This results in increased thermal conductivity 	[30] [31]
Internal fins	<ul style="list-style-type: none"> Another archetype for performance improvement is using internally finned structure Internal fins should be used 	<ul style="list-style-type: none"> Use of fins increases the thermal conductivity and hence the heat transfer. Xuejio et.al found an optimum Length to Radius ration of 0.75. They used a total of 6 fins and found more than 50% decrease in discharging time (3600 s as compared to 770 s without fins) 	[32]
PCM layer thickness	<ul style="list-style-type: none"> PCM layer thickness is essential indicator for Solar PCM System design 	<ul style="list-style-type: none"> Large PCM thickness tends to increase overall volume of the system while small PCM thickness results in insufficient performance 	[33]

Solar irradiation and climate	<ul style="list-style-type: none"> Atmospheric conditions are the first most parameter that is considered for designing SPCMS 	<ul style="list-style-type: none"> Transition temperature, mass of PCM, estimate of solar irradiation etc. all are dependent on climate of a particular place 	[34]
Area of solar collector	<ul style="list-style-type: none"> Based on climatic predictions and energy storage demand, Area of a solar collector is a key parameter 	<ul style="list-style-type: none"> It ensures that sufficient radiation from sun will be absorbed and thermally stored for use at off-solar time 	[35] [36]

2.2 Key Performance Indicators

As formerly explicated, Solar PCM Systems have a lot of ground to cover when it comes to their performance. Therefore, a comprehensive knowledge of all possible parameters that could affect the performance of these systems is indispensable. The subsequent sections discuss in detail about the technical and economic indicators that can significantly improve the performance of solar PCM Systems.

2.2.1 Thermal Performance Indicators

Mazhar et al. [37] carried out experimental investigation to study the performance of corrugated pipe in a PCM to harness grey water (GW).

The best option for heat transfer is to boost heat transfer coefficient. A thermal performance factor TPF1 is introduced to assess the performance of pipe, which is basically a measure of surface enhancement and defined as:

$$TPF1 = \frac{Nu_{corrugated}/Nu_{plane}}{(f_{corrugated}/f_{plane})^{1/3}}$$

It is concluded that the corrugated pipe with lower pitch length is not preferable. Moreover, the performance of corrugated pipe increases at lower mass-flow rate. Another important outcome is that all the TPF ratios are less than 1 as compared to plane pipe.

As TPF1 is a measure of the surface and not the thermal enhancement, so another thermal performance factor TPF2 is defined as:

$$TPF2 = \frac{\text{Heat transfer at the pipe interface}}{\text{Pumping power}} = \frac{\dot{Q}_{corrugated} / \dot{Q}_{plane}}{\frac{\dot{V}\nabla P_{corrugated}}{\dot{V}\nabla P_{plane}}}$$

According to this factor, higher pitch length is preferable. As compared to TPF1, high mass-flow rate with high rib height is more favoured. Moreover, for freezing the performance varies linearly with the variation of mass flow rate as compared to parabolic behaviour for melting.

Mahboob et al. [38] performed the experiments to study the effect of aspect ratio on the performance of a latent thermal storage unit for solar thermal applications. The experimental set-up consisted of three cylindrical storage tanks with different aspect ratios (height to diameter) 320 mm: 330 mm for 1:1, 560 mm: 250 mm for 2:1 and 720 mm:240 for 3:1. PCM balls are placed in the top 50 mm and bottom 50 mm space.

When the water in storage tank is stratified, the efficiency of TES and solar collector system increases. Stratification of water in tanks is produced by the difference in density between hot and cold water. Hot water comes at the top while the cold-water flows to the bottom. Richardson number is primarily used to describe stratification and is estimated by the following equation.

$$Ri = \frac{g\beta H[(T_{H-in}) - (TLb)]t}{v_{sf}^2}$$

$$v_{sf} = \frac{V}{\pi r^2}$$

It is concluded that stratification is influenced by PCM balls in storage tank irrespective of aspect ratio. The increase in stratification level increases the instantaneous heat transfer rate. The cumulative heat transfer decreases with time as the aspect ratio increases. The Richardson number also depicts resistance of PCM balls and it increases throughout the charging process especially with aspect ratio 1:1.

2.2.2 Economic Indicators

With the increasing fuel and electricity prices, there is a need to reduce the energy consumption by buildings. Researchers are working on designing economically efficient systems for heating/cooling purposes. There has been a lot of work on PCM integrated systems which have proved efficient in saving energy. Xiangfei et al. [39] experimentally

analyzed a hybrid system of PCM wallboards, with magnificent thermal and mechanical properties, integrated with a solar thermal system. The result showed 44.16% reduction in daily energy consumption. Saafi et al. [40] worked on a brick wall with PCM impregnated on the inside and outside surface and studied the energy saving potential of the system. They came up with the conclusion that the outside surface of the brick wall with PCM applied on it delivered a better energy efficiency. There has been researches on single or multiple layer configuration of PCM and results showed that multi-layered layout has better energy saving than single-layer layout [41][42]. The local climate conditions also affects the energy saving potential of a PCM-integrated building to some extent, with energy saving ranging from less than 1% [41] to up to 90% [43]. Sovetova et al. [44] assessed the energy efficiency performance of PCM integrated residential buildings in eight different cities with thirteen different PCMs with the help of Energy Plus software. There was variation in the reduction of energy consumption in the targeted cities from 17.97% to 34.26. Qu et al. [45] studied the influence of four parameters on energy saving and found that with proper selection of PCMs in accordance with the climatic conditions, considerable energy saving rate can be achieved with maximum limit up to 34.8%.

Morshed et al. [46] investigated the energy saving potential of PCMs in eight major Australian cities which represent six climate zones. The results showed 17-23% annual energy saving in the studied house depending on local weather. Haukeer et al. [47] evaluated the performance of PCM wallboards in air-conditioned buildings with summer and winter climate conditions. Different room locations on the middle floor of a building were studied. The results concluded that in summer, east and west wall has the highest energy saving rate, which can reach 27.78% in the east wall model. In winter, south wall has the highest efficiency, which can reach 96.2%. the room with south. PCM wall had the fastest payback period of 21.65 years. Juan et al. [48] studied the solar heating system with PCM storage tank and compared it with conventional water tank heating system for energy saving. The results show a 34% increase in energy saving capability. Paul Devaux [49] studied the PCM underfloor heating systems, and his analysis showed great potential of peak load shifting. He recorded 32% and 42% saving in energy and cost, respectively. Calise et al. [50] made a dynamic simulation, economic, and energy comparison between building integrated photovoltaic (BIPV) and building integrated photovoltaic/thermal (BIPV/T) collectors in TRNSYS. A payback period of 4.5 years was achieved using BIPV systems. This proves that the BIPV-based system was more energy efficient than the BIPV/T-based systems.

Researchers have used different tools to measure the economic impact of the PCM solar systems. They have calculated the energy saving, cost saving, electrical efficiency, payback period etc. Table 2 shows some of these parameters calculated in different literatures.

Table 2: Energy and Economic savings in different literatures

PCM	Site	Energy saving (kW/year)	Payback period (year)	Reference
BioPCM@™ M91	Nicosia	20.567	14.5	[51]
PCM27	Hong Kong	3798.34	30.09	[52]
PCM23	Australia	4833.33	-	[46]
PCM29	Iran	2969.65	42	[53]
PCM-enhanced insulation	Miami	19,954	7	[54]
TIM-PCM	Paris	668.8	22	[55]
n-hexadecane	Seoul	326.36	6.88	[56]
n-heptadecane	Seoul	312.18	6.80	[56]
n-octadecane	Seoul	205.37	8.38	[56]
25# Paraffin	China	-	3.32	[39]
Dupon Energain	Aveiro	-	41	[57]
BioPCM® M51	Aveiro	-	18	[57]
BioPCM® M91	Aveiro	-	26	[57]

2.3 Solar Integrated PCM Systems

SPCMS are confronted by their economic feasibility, therefore, immense caution must be taken while designing these systems. The forthcoming section extensively reviews the design, performance, thermal efficiency, energy savings and the studied variables of active and passive SPCMS.

A general flow diagram of SPCMS is shown in Figure 3:

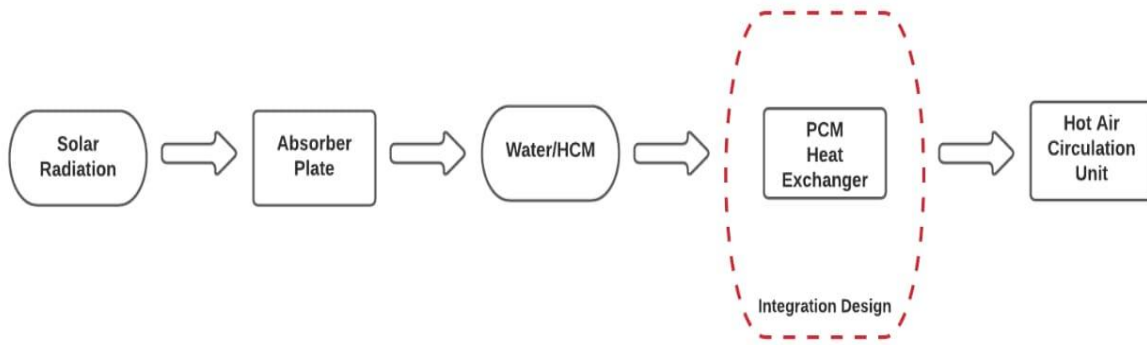


Figure 3: Flow diagram of SPCMs

Solar Integrated PCM systems can be classified as active solar PCM systems and passive solar PCM systems. Active solar PCM systems include some active (power consuming) components, whereas, Passive solar PCM systems do not have any power consuming components.

Figure 4 shows a generic schematic of solar PCM systems.

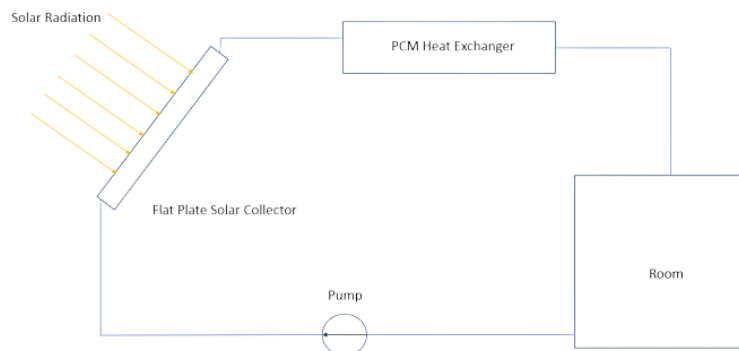


Figure 4: Schematic of solar integrated PCM systems

2.3.1 Active Systems

SPCMS requiring auxiliary components for their operation are referred to as active solar PCM systems. A detailed review of active SPCMS is tabulated in Table 3:

Table 3: Summary of review papers in active domain

Subject	Overview	Outcome	Ref.

<p>PCM storage for solar DHW using a water pump</p>	<ul style="list-style-type: none"> • The system comprised of a solar collector, pump, tank, water pipes, circular PCM tubes and an auxiliary heater • Solar collector warms the water for distributed heating which in turn transfers thermal energy to composite paraffin PCM present in circular tubes in the water tank. • Energy stored in PCM prevents auxiliary heater from turning ON and saves electricity consumption at night by releasing its energy to incoming cold water • A simple energy balance approach was used to obtain outlet temperature of water and useful heat gain. The problem was considered one-dimensional and due to the use of composite PCM of good thermal conductivity, lumped capacitance approach was used. 	<ul style="list-style-type: none"> • Annual solar energy delivered to the consumer increased from 6457 MJ without PCM to 6692 MJ With PCM • Annual electricity backup for auxiliary heater reduced from 843 MJ to 723MJ • Collector efficiency using PCM increased from 45.2% to 46.5% 	<p>[58]</p>
<p>Compact PCM solar collector using a pump</p>	<ul style="list-style-type: none"> • The study aimed to check the relation between water flow rates and useful heat gain, heat transfer coefficient for charging of PCM and distribution of freezing and melting fronts of PCM during charging and discharging process. • The system consists of an absorber unit container made of steel. The absorber plate is tilted at 45 degrees. • The absorber container is filled with PCM and copper tubes containing water are embedded within PCM. Pump is used to circulate water in the absorber container • Sides of the container are insulated using polyurethane and wood. During charging process the glazing of absorber plate is exposed to sunlight and is covered with insulation during discharge time to prevent top losses to the environment • An analytical model using energy balance in one direction was used to find heat transfer 	<ul style="list-style-type: none"> • During charging process solid-liquid profiles are similar. • During the discharging process, the solid-liquid profile is elliptic for sensible phase and circular during latent phase. • Useful heat gain increased with increased flow rate. • Useful gain tends to decrease with time • The heat transfer coefficient decreases as the distance from the top decreases. • At the top layer, heat transfer coefficient increases with time due natural-convection currents in melted layer. 	<p>[13]</p>

	coefficient as a function of distance as well as useful heat gain.		
DP-SAH using capsules of PCM	<ul style="list-style-type: none"> The goal was to numerically and experimentally study the thermal performance of a double pass solar air heater (DP-SAH) having paraffin wax capsules integrated with finned absorber plate. Focal point is to study the effect of solar irradiance and air flow rates on performance of DP-SAH. Air is made to flow over both sides of absorber plate by a 65W axial fan. The apparatus consists of a DP-SAH, glaze cover, finned absorber plate, fan, artificial solar simulator, and sensors for measuring flow rates, several k-type thermocouples, and solar intensity measurement sensors. Energy balance was used to find useful gain and top loss from collector plate while finite element scheme based on Navier stokes momentum equation, continuity equation and energy equation was employed to simulate three-dimensional forced convective fluid flow. 	<ul style="list-style-type: none"> All numerical and experimental results differ at max by 7% Their research showed that increased air flow rate results in delay of melting period and decrease melting temperature of paraffin wax It was shown that freezing time has an inverse relation with flow rate 	[59]
Solar double slope PCM glazed roof	<ul style="list-style-type: none"> Glazed roofs are constructed for better lighting but due to poor insulation, they result in thermal discomfort. The focus of the study lies in addressing this issue. The solution proposed is to embed the double sloped glazed roof with and without PCM sandwiched in between. The performance of both concepts would be 	<ul style="list-style-type: none"> The average error between actual and numerical results were under 7% Results showed that PCM sandwiched double glazed roof provide better thermal performance as compared to hollow double-glazed roof 	[60]

	<p>compared.</p> <ul style="list-style-type: none"> • The effects of changing different parameters of PCM and glazing such as roof angle, PCM layer thickness, different PCM melting temperature, different PCM latent heat and different PCM melting temperatures were also studied • Air is passed on both sides using fans and this air warmed through forced convection is circulated in room to achieve thermal comfort zone. • For numerical modelling, radiative heat transfer is ignored, material properties are assumed to be independent of temperature, glazing and PCM is assumed to be homogeneous and optical properties are assumed to be independent of wavelength • Heat diffusion equation and Fourier law is used to obtain equation of heat conduction. From this equation, the problem is assumed to be one-dimensional along the thickness direction and internal energy generation is neglected which leads to a simplified equation. • A numerical model was also proposed on FLUENT module of ANSYS which simulated three-dimensional transient flow of the actual system modelled on CAD. Energy and momentum equations were enabled for the simulation. Energy residual monitor was set to 1e-06 and time step was set to 10s. 	<ul style="list-style-type: none"> • It was also shown that increasing the layer thickness of both glazing and PCM results in better thermal performance • Under climatic conditions of Wuhan, phase change temperature between 26-30 degrees provide better thermal performance • Thermal performance also increased by choosing a PCM of high latent heat and by decreasing the angle of roof glazing. 	
--	---	---	--

<p>Active slab containing PCM integrated to solar air collector</p>	<ul style="list-style-type: none"> • Study of a horizontal concrete slab of a building construction having macro encapsulated PCM channels fitted inside to decrease the energy requirements of the building. • The reason behind the installation of PCM within the slab is to eliminate entirely the energy losses to environment. • The model was constructed to be tested under real time weather conditions of Spain. • The apparatus consisted of a small cubical building having a horizontal concrete slab having macro encapsulated PCM channels. The slab has a passage of air circulation to forcefully melt the PCM using the air warmed through solar air heater. • A control system was employed to control the melting of PCM through warm air coming from solar air heater. 	<ul style="list-style-type: none"> • In multiple testing, incomplete melting was observed which suggests exploring in detail the ratio of size of solar air heater and the quantity of PCM. • Complete melting of PCM showed energy savings of 55%. Even if the PCM melts partially it results in energy savings of about 20%. • They suggested that optimization of control system algorithm can increase the energy savings further. • On average weather conditions, 40% energy savings were achieved. 	<p>[61]</p>
<p>Preheating of the ventilation air using solar PCM</p>	<ul style="list-style-type: none"> • They aimed to supply pre-heated ventilation air using solar heat stored beneath a ventilation window in a PCM. • The objective of the study was to maintain thermal comfort of the room during ventilation at minimum cost. • The system was studied both experimentally and numerically. • Non-linear thermal properties of PCM, heat transfer model, and buoyancy derived laminar flow models, Navier stokes equation, continuity equation were integrated to numerically model the whole system. • The apparatus consisted of full scale hot and cold rooms. The cold room maintains its temperature through a cooling coil. PCM heat exchanger is in between hot and cold rooms 	<ul style="list-style-type: none"> • Close correspondence between numerical and experimental results was found which rationalised the use of this numerical model for further optimisation of the system. • The error between experimental and numerical studies never exceeded more than 6% in any aspect. • The heat released through fully charged PCM was 93.31 Mj/m^3 • The system was exposed to 550 W solar charging for 6 hours 	<p>[10]</p>

	<ul style="list-style-type: none"> • In the experiment, hot room is ventilated through the air from cold room. The cold room air passes through PCM heat exchanger which is being charged with an artificial sun and gets warm. • The air enters from the bottom of heat exchanger, in between the PCM plates and finally enters the hot room through the ventilation cavity of a double-glazed ventilation window. • The air passes through the heat exchanger only when solar radiation is less than 200 W/m^2. Otherwise, air directly goes into the room because it is sufficiently warmed by sun itself that there is no need for pre-heating. • Exact configuration can be used for cooling requirements in which discharged PCM gets charged by absorbing heat from the room where cooling is needed. 	<ul style="list-style-type: none"> • They studied the relation of various depths of PCM tubes with charging and discharging time along with the relation of gap between the tubes • They found maximum melt of PCM with 90mm PCM plate with a 90.2% melt fraction contrary to 59.5% and 69.8% from 100mm and 110 mm plates. • They observed that depth of PCM plate does not affect the discharge time. Nonetheless, with 90mm plate depth, the energy released was exactly 93.31 Mj/m^3 • The discharge rate decreases with increase of gap between the plates but not very significantly indicating that energy released is a dominant factor of total solar energy absorbed by PCM and not the air gap. 	
<p>Hybrid PCM system of an active composite wall</p>	<ul style="list-style-type: none"> • The system comprised of passive PCM wallboard linked with active solar thermal system to constitute a hybrid system. • In this study, expanded perlite-based composite was used as a phase change material and was integrated into a wallboard and then incorporated with solar thermal system by capillaries. 	<ul style="list-style-type: none"> • Incorporation of PCM wallboards with solar thermal system produced satisfactory results. • Thermal conductivity increases by 109.09% with the addition of aluminium powder in wallboard II. 	[39]

	<ul style="list-style-type: none"> Two PCM wallboards were made using newly made PCM particles, styrene acrylic emulsion, environment friendly paint, and fibre glass. Wallboard I was plain while wallboard II had grooves where capillaries were installed. Additional aluminium powder was used in wallboard II to enhance thermal conductivity. Two same sized rooms were prepared to conduct three series of experiments. Both rooms comprised of a heat exchange tank and were connected with solar collectors. 	<ul style="list-style-type: none"> PCM wallboard has maximum pressure endurance of 98N and maximum flexure strength 0.41Mpa, with 7.85mm deflection, which indicates high strength of wall. Daily energy consumption was reduced 44.16% using this hybrid system. 	
<p>PCM integrated solar chimney</p>	<ul style="list-style-type: none"> The study intended to experimentally study the effects of PCM on the performance of two different solar chimney prototypes The first prototype analysed the behaviour of Rubitherm RT44 PCM panels on simple-build solar chimney. The second prototype was a modified version build according to design of SPA (Solar Platform of Almeria). Experiments were conducted with and without PMC comprising 6h long seven consecutive phases. The cycle starts with initialization, then charging of PCM, air circulation and maintaining of heat source, and then removal of air source. In last 3 phases it repeats the phase 1, 3 and 4. High level instrumentation system was used to measure the parameters like air temperature, surface temperature, mass flow rate etc. 	<ul style="list-style-type: none"> Although there was incomplete fusion of materials within the panels, the outcomes of the experiment were obtained. Additional layer helped avoid heat loss across the chimney and PCM panels provided thermal inertia. After a charging period of 6h, an average ventilation rate of above 70 m³/h can be attained with a low gain of 550W/m² provided by a series of 7 halogen lamps. During the discharging period solar chimney provided a slower decrease in ventilation rate with an overall higher ventilation rate. 	[62]

<p>Dual-air-channel PCM system with solar wall</p>	<ul style="list-style-type: none"> • The multi-functional dual-air-channel solar wall scheme with PCM consists of glass cover, absorbing plate, PV cells, water pipes, pump, cycle pump, tank, PCMs, Insulation later, wall and the vents. • In an entire year, the system works on three modes: winter mode, summer mode and transition season (spring and autumn) mode. • In winter mode, in daytime, heat is transferred between absorber plate and air via convection. The heated air charges the PCM. In night-time, heat stored in PCM is used. • In summer mode, in daytime, pump is used to circulate water which gains heat from absorber plate. The heat of air is absorbed by PCM, and it passively cools the air at night. • In transition season mode, in daytime t is same as in summer mode and in night-time is same as in winter mode. <p>A mathematical model of whole system is formulated for validation.</p>	<ul style="list-style-type: none"> • In each working mode, the system accomplished good electrical and thermal performance and continuous indoor space heating was improved during night-time. • The correctness of established model was found acceptable through the model validation. • Performance of the system can be made better with a proper increase of the PV cells coverage and channel height. • The appropriate transition temperature range of PCM is 19-21C in the winter days and 22-24C in the transition season days. This will provide better continuous space heating performance during nocturnal hours. 	<p>[63]</p>
<p>Solar aided PCM based Space heating</p>	<ul style="list-style-type: none"> • The goal was to investigate the thermal performance of a solar-aided latent heat source store for space heating by heat pump. • The experimental setup consists of flat plate solar collector, thermal energy storage tank filled with encapsulated PCM, a heat pump with water sourced evaporator and air-cooled condenser and a room for heating. • Two modes of operation were investigated. The first mode occurs when water receives solar heat from solar flat pate collector. This water goes to energy storage tank, a part of this energy releases to storage tank. Then it is used by water sourced evaporator of the heat pump. 	<ul style="list-style-type: none"> • The instantaneous total of percentages of PCM in transition and liquid range is always 100 % • The thickness of pipes should be less to minimize the energy storage in the walls of pipe. • In the beginning, the outlet temperature of tank is low which insisted that pipes od short length and tank with small hight should be selected. 	<p>[64]</p>

2.3.2 Passive Systems

SPCMS which do not require any auxiliary components for their operation are referred to as passive solar PCM systems [65][66]. Table 4 extensively reviews passive SPCMS.

Table 4: Summary of review papers in passive domain

Subject	Overview	Outcome	Ref.
PCM in gypsum boards	<ul style="list-style-type: none"> The system consisted of gypsum board incorporated with PCM, minerals and admixtures to improve working properties. The melting range of PCM is between 25 °C and 28 °C with a constant heat and cooling rate of 2 K/min. Two similar experimental chambers were made, the walls of 1st chamber were covered with ordinary plaster board while the walls of 2nd chamber were covered with PCM wall board. 	<ul style="list-style-type: none"> A reduction in temperature of about 3 K was achieved in test chamber having walls of PCM plaster board as compared to test chamber without PCM. 	[67] [68] [69]
PCM in concrete	<ul style="list-style-type: none"> An experimental investigation carried out to study the performance of PCM concrete set-up. The system comprised of four testing chambers, two with PCM concrete floor and two with normal floor. Solar irradiation is the only heat source. 	<ul style="list-style-type: none"> This research indicated that temperature fluctuation could be decreased by this technology. Since the PCM floor was directly exposed to solar irradiation in this experiment. To implement this set-up in practice is difficult because floor is always covered with tiles, wood etc which minimizes direct contact of solar irradiation and PCM. 	[70] [71]
PCM in bricks	<ul style="list-style-type: none"> The study was carried out to investigate the potential of PCM as passive solution in bricks to reduce the time delay in internal and external conditions and fluctuations. 	<ul style="list-style-type: none"> The results showed that time delay of 3 h could be achieved by using brick wall with PCM. 	[72] [73]

	<ul style="list-style-type: none"> The set-up was comprised of two walls of clay, one with microencapsulated PCM and without PCM. Climatic chamber was used to test the walls, with one side having external boundary condition and the other with free floating condition. The PCM used was RT18 having melting temperature of 18 °C. 	<ul style="list-style-type: none"> Thermal amplitude decreased from 10 °C. with PCM wall to 5 °C without PCM wall. 	
PCM based free cooling	<ul style="list-style-type: none"> An experimental investigation was performed to study the potential of PCM based free cooling i.e., storing energy at night-time in flat modular type heat exchanger incorporated with PCM and using same energy for cooling in daytime. The system is consisted of a cabin with an area 64 ft². The temperature variations during charging and discharging were investigated. The heat exchanger was made up of 10 rectangular stainless-steel panels. 76 kg of HS 29 PCM with transition temperature of 28 - 29 °C was used. 	<ul style="list-style-type: none"> The results revealed that temperature could be reduced to 2.5 °C in the cabin. At initial stage of charging, instantaneous heat rate of 0.35 KW was noted which reduces to 0.2 KW after 500 min. It is also understood that temperature driving potential between phase change temperature and ambient temperature is the major design parameter. 	[74]
PCM Trombe wall	<ul style="list-style-type: none"> Trombe wall consists of a glass glazing and a brick wall with an air gap of 4-5 inches in between. The air gap traps heat during the day and later at night is dissipated into the room through the wall. PCM is used in the walls for better heat storage. The study was conducted on a PCM Trombe wall and a conventional concrete wall. Paraffin with mixed metal shavings was used for increased overall conductivity and efficiency. The goal was to achieve low mass and high efficiency walls. 	<ul style="list-style-type: none"> Conclusion was made that thermal resistance of the solar thermal wall should be as low as possible. In comparison with concrete walls, paraffin-metal mixtures offered a 90% reduction in storage mass and a 20% increase in thermal efficiency. 	[75] [76] [77]

<p>PCM Shutter</p>	<ul style="list-style-type: none"> The goal is to increase thermal performance of shutters placed outside of windows in warming a cold room at night using thermal storage. Thermal performance of a test cell (1m × 1m × 1m) is observed with and without PCM. CG Lauric Acid with a melting point of 49 °C was used as a storage material. 	<ul style="list-style-type: none"> The heat storing capacity of the cell when used at night increases up to 4 °C for 4-5 hrs due to presence of PCM. 	<p>[78]</p>
<p>PCM after mosaic tiles</p>	<ul style="list-style-type: none"> A panel of PCM is placed after layer of mosaic tiles and cement of 0.005 m thickness with a melting point of 21.7 °C. The system is used for cooling the room with a goal of higher efficiency. 	<ul style="list-style-type: none"> Cooling energy savings achieved annually were low (2.9 %). 	<p>[79]</p>
<p>Air-based heating system</p>	<ul style="list-style-type: none"> The performance of air-based solar heating system was studied using PCM. The goal was to work out the effect of latent heat and melting temperature of PCM on the air-based solar heating system. 	<ul style="list-style-type: none"> The selection of PCM should be made based on its melting point and latent heat. The air-based heating system utilizing sodium sulphate decahydrate as a PCM requires roughly one-fourth the storage volume of a rock bed and one-half the storage volume of a water tank. 	<p>[80]</p>
<p>PCM in ceilings</p>	<ul style="list-style-type: none"> The experiment was carried out using sun reflectors to direct the solar energy on to PCM incorporated in the ceiling void for a space heating system. The system had a large area for heat storage without needing large volumes for storage medium that would be required with sensible heat storage. The goal was to prevent heat loss. 	<ul style="list-style-type: none"> This system had the potential to recover 17–36% of heat lost over the initial gains. 	<p>[81] [82]</p>

2.4 Solar PCM Optimization Techniques

Thermal performance of solar PCM systems being a challenge beseeched the researchers to optimize these systems for best performance. Following techniques are applied for optimization of solar PCM systems:

- Analytical optimizations
- Numerical optimizations
- Algorithmic optimizations

The forthcoming section extensively reviews analytical and numerical optimization techniques for various performance parameters

2.4.1 Theoretical Optimization

In this technique, fundamental equations of the field of study are modelled in accordance with the specific problem at hand. For instance, in solar PCM systems, fundamental equations are the energy balance equation, continuity equation, heat diffusion equation, Fourier law etc. [57][83]. Once the parameters and boundary conditions of the problem at hand are compensated into these equations, we can solve them analytically. Consequently, by solving the equations mentioned in above table numerous times with different magnitudes of performance parameters results in optimization of the system. Although nowadays it is convenient to use algorithm or simulation-based techniques for optimization, a few examples of analytical optimization are discussed below. Consequently, by solving the equations mentioned in above table numerous times with different magnitudes of performance parameters results in optimization of the system.

Xioa et.al. [56] optimized a solar system of PCM storage inside a lightweight construction room. They employed a theoretical approach for optimization of this system. For modelling purpose, following assumptions were made for simplification of this analysis:

- Sensible thermal capacity was neglected and high latent heat of PCM was assumed at a single- phase change temperature.
- A single heat transfer coefficient was assumed for both radiative and convective heat transfer.
- Owing to small thermal conductance resistance inside the wall, temperature inside the wall is considered uniform.

Selection of phase change temperature is crucial for the performance of the system. For an optimum phase change temperature energy stored and released during a cycle should be equal. Following energy conservation equation was employed for optimum phase change temperature.

$$m_i \frac{dH_i}{dT} = h_{in} \cdot A_i \cdot (T_a - T_{m,i}) + Q_{rj} + Q_{r,in,i}$$

where subscript ‘i’ refers to ith PCM panel. Assuming constant enthalpy over the cycle (taking dH_i Term =0) and integrating the above equation on both sides we get the equation for melting temperature

$$T_{m,i} = T_a + \frac{\int (Q_{r,i} + Q_{r,in,i}) dT}{h_{in} \cdot P \cdot A_i}$$

The above equation shows that optimum melting temperature depends on room temperature and the absorbed solar radiation.

Lamberg et.al. [84] studied a solar PCM system with PCM encapsulated in a housing with internal metallic fins. This system is shown in Figure 5:

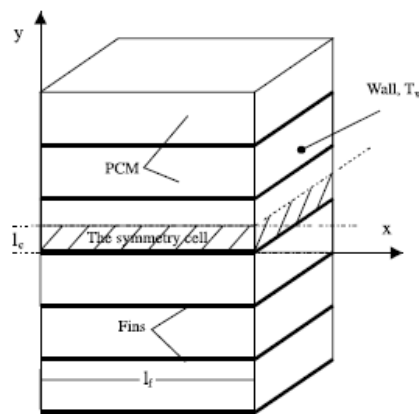


Figure 5: PCM Embedded in a Wall [84]

Two-dimensional problem is not possible to solve analytically, therefore a one-dimensional model was proposed with simplified assumptions.

The governing equation of the model is one-phase Stephan heat equation which is written below

$$\frac{\partial^2 T_s}{\partial x^2} = \frac{1}{\alpha_s} * \frac{\partial T_s}{\partial t}, t > 0, 0 \leq x \leq l_f$$

and the boundary conditions are:

$$-(\rho L)_s * \frac{\partial S_x(t)}{\partial t} = -k_s * \frac{\partial T_s(S_x, t)}{\partial x}, t > 0$$

$$S_x(0) = 0$$

$$T_s(S_x, t) = T_m$$

$$T_s(0, t) = T_s(l_f, t) = T_w$$

For fins, an energy balance was written as:

$$E_f = -q_x + q_{x+dx} - q_c$$

After applying the boundary conditions, tedious manipulation and solving the above equations, the solution of the following form was obtained for the location of solid-Liquid interface:

$$S_y = l_c \gamma$$

Where l_c is the length from where convection is taking place and

$$\gamma = \sqrt{2\zeta k \tau \lambda^2 \theta}$$

And finally, the equation for fraction of solidified PCM is:

$$\epsilon = \frac{2S_x(L_c - D - S_y) + S_y L_f}{(L_c - D L_f)}$$

This equation can be used to increase the fraction of solidified PCM by varying the parameters on the right side of this equation. Thus, this equation optimizes the solidification process. The subscripts and nomenclature have been defined at the start of the paper.

2.4.2 Numerical based Optimization

Numerical models and their solutions using computer software are most convenient approaches used nowadays for optimization of solar PCM systems. These solutions are mostly based on finite element method (FEM), finite volume method (FVM) and finite difference method (FDM). These methods discretize the problems into smaller elements and provide a solution converged within very low error bounds. Among the prior mentioned methods; finite element analysis (FEA) is most preferred due to its capability of sampling at arbitrary space locations instead of chronologically following a rectangular grid as in FDM [85].

The principle of such solutions is that certain non-linear higher order partial differential equations such as Navier stokes equation, energy equation etc. which can model the problem at hand are given boundary conditions and inputs. Then whole domain of the problem is discretized in smaller elements and FEA, FEM, FDM are used to provide large set of equations whose common solution is required. Then using numerical approaches like RK, gauss elimination, newton method, quassi-newton method etc. the solution of these equations is approximated within defined error bounds. The forthcoming section presents some numerical and simulation-based optimizations done by various researchers. The approach is generally similar which includes developing of a CAD model. Importing of that cad model into a commercial software such as ANSYS FLUENT, COMSOL, Autodesk CFD etc. and then modelling that system using above mentioned equations and finally calculating desired parameters and post processing of the results.

Allouhi et.al [33] analyzed an integrated collector storage solar water heater. The architect of the system is shown in Figure 6:

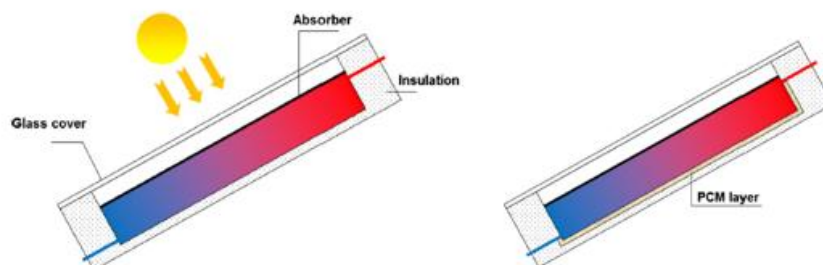


Figure 6: ICSSW with and without PCM [33]

The goal of this study was to optimize melting and solidification of PCM layer at the bottom of **Error! Reference source not found.** by varying the design variables in a numerical model. Ansys Fluent was used to numerically solve this system. A cad model like the schematic shown in **Error! Reference source not found.** was developed and meshed using Gambit software. The number of cells were 29,925. The analysis was set to 2-D unsteady laminar incompressible flow and a time dependent heat flux was applied at the top of the absorber plate using a user-defined function to model solar irradiation. Water inlet temperature was set to 298 K and velocity of water was chosen such that Reynolds number is less than 200. The magnitude of solar flux was being updated on hourly basis using TRANSOL program according to Moroccan conditions. Following were the governing equations of the numerical model:

- Enthalpy formation module for melting and solidification
- Momentum equation
- Continuity equation
- Energy equation

After fabricating the above-described numerical model. They solved that model several times with different operating conditions like varying mass flow rate, with or without PCM, different solar irradiation and inlet conditions. By just changing the parameters in the model they were able to optimize the mass flow rate, PCM layer thickness etc. This numerical model also enabled them to observe and optimize the melted fraction of PCM.

A PCM system consisting of a sleeve in the form of a concentric tube heat exchanger was studied by Wang et.al in 2015 [86]. PCM in solidified form was filled in the outer tube of the sleeve. A numerical model was prepared for the optimization of melting of PCM by varying geometry of fins, angle between successive fins and melting without fins. Different geometries analyzed for optimization are shown in **Error! Reference source not found.**

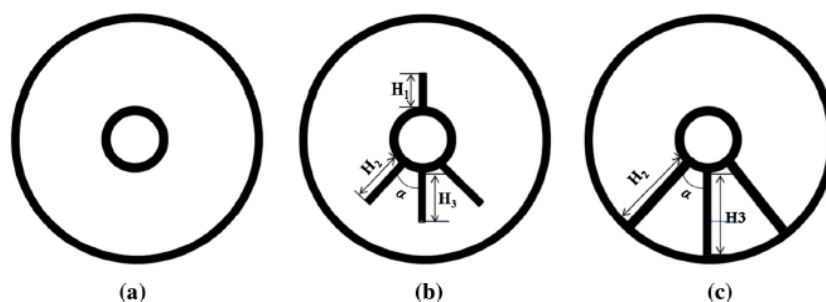


Figure 7: Different Configurations of PCM Sleeve Tubes (a) Without Fin ; (b) Half Fins ; (c) Full Fins [86]

The geometry without fin, with half fin, with full fins had 4732, 4731, 4764 grids respectively. Ansys Fluent was used for solving the numerical model. Due to the symmetric nature of the geometry, only half geometry was considered for saving computational time. Since liquid-solid interaction was involved, so, melting/solidification module was used. For modelling of phase change process enthalpy model was used. Moreover, continuity equation, momentum equation and energy equations with power law differencing scheme and a time step of 0.05s was used. PRESTO scheme was used for pressure correction. A convergence criterion of 10^{-5} for continuity and velocity whereas 10^{-9} convergence criteria for energy equation was used. After modelling the system according to the above-mentioned settings and modules, and boundary conditions, it was solved for the geometries shown in Figure 4 to see the optimized configuration. Numerical results agreed with experimental results which articulates the use of numerical models for optimizations. This numerical optimization suggested that optimum angle between consecutive fins is between 60-90 degrees. Moreover, melting time was least with half fin geometry and the combined effect of angle optimization and geometry optimization lead to a 49.1% decrease in melting time.

Chapter 3: Design and Calculation of PCM Heat Exchanger

Design Methodology is discussed in this section which resulted in the final model of heat exchanger represented in Figure 8. The model was rendered on KeyShot 9.0 and suitable skin layer was selected for better representation.

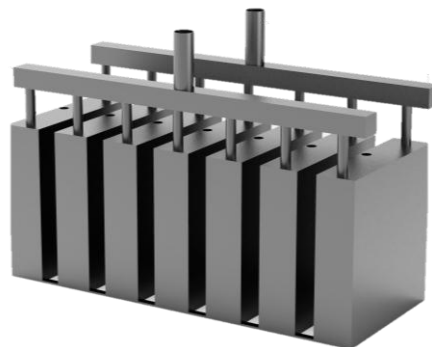


Figure 8: Heat Exchanger Design

3.1 Design Approach

The purpose of PCM heat exchanger is to passively transfer heat from the phase change material (PCM), which stores latent energy, to air in the room. First step towards the design of the system is the selection of type of heat exchanger.

There are different types of heat exchanger designs. A shell and tube heat exchanger design is used to enclose PCM in the shell and circulate hot water in the tubes. Heat is transferred from the hot water to the PCM. PCM is charged i.e. it stores the heat mostly in latent energy. For heating water, low grade thermal energy is required that can be taken from any renewable energy source. Solar energy could be used to heat up water to a higher temperature than the transition temperature of PCM. Concentrated solar collector with reflective surface are most appropriate to be used to concentrate direct sunlight at small areas of water to raise its temperature. To circulate hot water in the heat exchanger, a submersible pump is used. The pump is placed inside the hot water tank. Flexible plastic pipes, that can withstand high temperature, are used to direct hot water from submersible pump to the inlet of heat exchanger and direct cold water from heat exchanger outlet back to the water tank. Stainless steel fitting clamps are used to clamp the pipes to heat exchanger inlet and outlet. Forced fan is used to assist in transferring heat from PCM to air by forced convection.

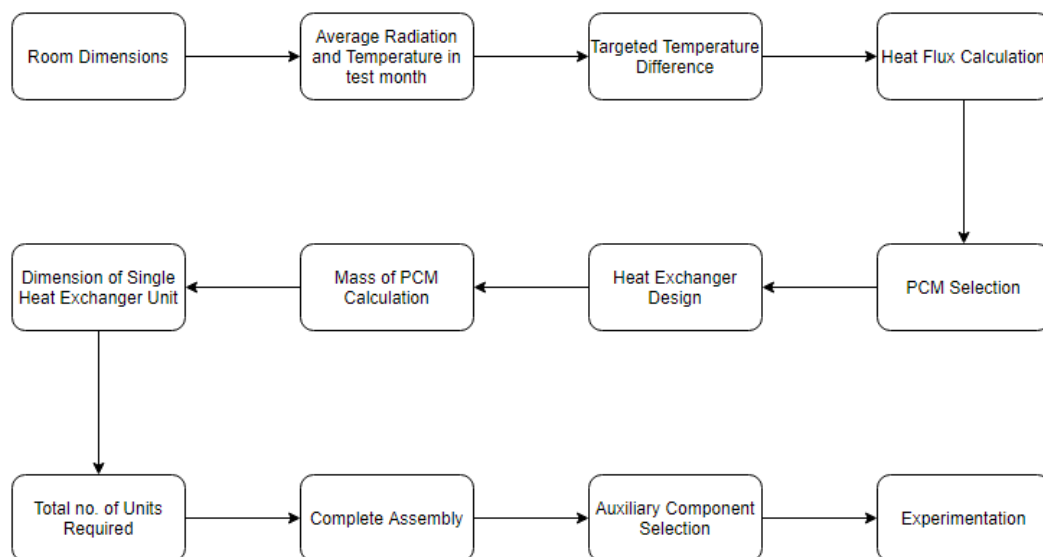


Figure 9: Flow diagram of design Approach

3.2 Design Requirements

To commence with the design approach, the dimensions of a feasible small-scale control room for experimentation of PCM heat exchanger are specified. Test month is decided, and the average radiation and ambient temperature of that month are noted. A targeted temperature difference of 10°C is set to achieve in room according to thermal comfort zone of ASHRAE while keeping in mind the limitations of solar PCM systems due to their lower thermal conductivities. Heat flux required to raise the temperature in the control room to the targeted value is calculated using laws of convection.

PCM is then selected according to the design requirements and economical availability. Then the most important part is the design of a novice heat exchanger using theoretical and computational tools; encapsulating PCM in shell and water in tubes capable of augmenting the thermal conductivity of the system and heat transfer process through it. The heat transfer between PCM and the ambient air to achieve the calculated heat flux gives us the required mass of PCM. To encapsulate the required mass in the heat exchanger, the dimensions of a single heat exchanger unit are set, and the total number of units required are calculated. Auxiliary components used in the experimentation like pump, fan etc. are then selected according to the requirements. A submersible pump that can bear high thermal loads and has adequate pumping capacity required by our system is selected. Fan is selected that has enough flow rate to circulate air around the room. Finally, experimental configuration is set and experimentation is performed.

3.3 Material Selection

Mathematical modelling was done to reach on a suitable material as per requirements and availability in the region. Further details of the materials chosen for obligatory components are discussed in this section.

3.3.1 PCM

We have used Paraffin wax as PCM in our project. It is mainly used because it is economical and easily available. Paraffin wax has some limitations as its transition temperature is relatively higher in the range of 45°C to 50°C. An alternate option for PCM was L'Oréal alcohol with transition temperature of 25°C but it is much expensive i.e., it is Rs. 10,000/kg as compared to Paraffin wax which is Rs. 1,400/kg. The properties of Paraffin wax are given in the Table 5:

Table 5: Properties of Paraffin wax

Property	Value
Density	750 kg/m ³
Thermal conductivity	0.15 W/m.K
Latent heat	190 kJ/kg
Specific heat	2.3 kJ/kg/°C
Transition temperature	45°C - 50°C

3.3.2 Heat Exchanger

Heat exchanger is made of stainless steel. It is used because it is cheaper and has better strength. Although, copper has best conductivity, but it is expensive, so it is not used. Same is the case with brass. Mild steel is cheap but when in contact with water, rusting occurs which is a major problem. So, stainless steel is best among these.

3.3.3 Control Room

Walls, floor, and ceiling of the experiment room are made of tin. Tin is used because it is economical light weight and provides an airtight environment required for the testing. Styrofoam sheets are used to insulate the whole room for better results. Plastic sheet is used to wrap around Styrofoam sheets for firmly holding the sheets and adding to the insulation.

3.4 Room Design

For testing of solar PCM heat exchanger for indoor temperature stabilization, an experiment room is designed. Tin is used to make the room and mild steel is used for a frame at the bottom. The frame provides support and tires are attached at the bottom for east movement of the experiment room. To insulate the room, Styrofoam sheets are used around the walls. The dimensions of the room are listed in the Table 6:

Table 6: Room dimensions

Property	Value
Length	36 in.
Width	36 in.
Height	36 in.
Volume	46656 in. ³

3.5 Heat Exchanger Design

A rectangular shell and tube heat exchanger is designed encapsulating PCM in shell and water in tubes capable of augmenting the thermal conductivity of the system and heat transfer process through it. The mathematical calculations of the heat exchanger are done in Section 3.6 Calculations.

Heat exchanger consisted of seven units, a labelled unit is shown in Figure 10.

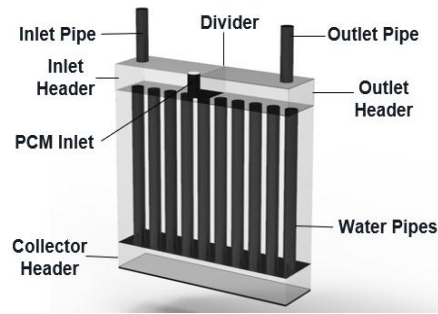


Figure 10: Unit Exchanger

3.6 Calculations

Average indoor temperature in Pakistan in winters is 12°C. We intend to increase the room temperature by 5°C up till 17°C. So, our $\Delta T = 10^\circ\text{C}$

Heat is transferred by free convection which has a convection coefficient $h = 7.5 \text{ W/m}^2\cdot\text{K}$

The area for this heat transfer is the whole surface of wall, $A = 0.9 \times 0.9 = 0.81 \text{ m}^2$

Hence, the thermal power needed to attain this temperature difference is given by the formula:

$$\dot{Q} = (h)(A)(\Delta T)$$

$$\dot{Q} = (7.5)(0.81)(10)$$

$$\dot{Q} = 60.75 \text{ W/s}$$

To find the thermal energy, we multiply the power with the discharge time. Discharge time varies in case of PCM from 2 hr to 8 hr. We take an estimated discharge time of 6 hrs. Table 7 shows the iterations for different discharge times.

For 6 hr.

$$Q = (\dot{Q})(t)$$

$$Q = (60.755)(6 \times 60 \times 60)$$

$$Q = 1312.2 \text{ kJ}$$

To supply this much energy from PCM to air, the mass of PCM required can be calculated using the equation:

$$Q = m_{\text{pcm}} \times h_{\text{fg}}$$

Where, m_{pcm} is mass of PCM and h_{fg} is latent heat of fusion of PCM which is 190 kJ/kg

So, mass of PCM required will be

$$m_{pcm} = Q/h_{fg}$$

$$m_{pcm} = 1312.2/190$$

$$m_{pcm} = 6.91 \text{ kg}$$

Hence, the mass of PCM required to raise the temperature of the room by 5°C is approximately 7 kg.

$$m_{pcm} = 7 \text{ kg}$$

Table 7: Iterations for mass calculation

Discharge Time (hrs)	Thermal Energy (KJ)	Mass of PCM (kg)
2	437.4	2.31
4	874.8	4.61
6	1312.2	6.91
8	1749.6	9.21

We have specified the dimensions of one unit of heat exchanger. The dimensions are listed in the Table 8:

Table 8: Dimensions of one unit of Heat exchanger

Property	Value
Length	2 in.
Width	6 in.
Height	8 in.

One unit contains 10 pipes of diameter $d = 0.4$ in.

Volume left for accompanying PCM is:

$$V = \text{volume of unit} - \text{volume of pipes}$$

$$V = (2)(6)(8) - 10\left(\frac{\pi}{4} \times 0.4^2\right)$$

$$V = 96 - 5$$

$$V = 91 \text{ in}^2$$

$$V = 0.0015 \text{ m}^2$$

Mass of PCM in one unit can be calculated as:

$$\begin{aligned} m &= (\rho)(V) \\ m &= (750)(0.0015) \\ m &= 1.125 \text{ kg} \end{aligned}$$

No. of heat exchanger units required are:

$$\begin{aligned} \text{No. of Units} &= \text{total mass} / \text{mass in one unit} \\ \text{No. of Units} &= 7 / 1.25 \\ \text{No. of Units} &= 6.22 \end{aligned}$$

So, the no. of heat exchanger units required are 7.

We need air passage between each heat exchanger. There are 7 units so there will be 6 air passages in between. The thickness of one air passage is 1 in. So, the total length of heat exchanger will be:

$$\begin{aligned} \text{Total length} &= \text{length of heat exchanger units} + \text{length of air passage} \\ \text{Total length} &= 7(2) + 6(1) \\ \text{Total length} &= 20 \text{ in.} \end{aligned}$$

Total volume of heat exchanger is:

$$V_{\text{total}} = (6) (8) (20) = 960 \text{ in}^3$$

Percentage of room occupied by the heat exchangers:

$$\begin{aligned} \% \text{ Of room occupied} &= \text{volume of heat exchanger} / \text{volume of room} \\ \% \text{ Of room occupied} &= 960 / 46656 \\ \% \text{ Of room occupied} &= 2.1\% \end{aligned}$$

The specifications of whole heat exchanger are summarized in the Table 9:

Table 9: Specifications of the Heat exchanger

No. of Units	7
Height of one unit	8 in.
Width of one unit	6 in.
Thickness of one unit	2 in.
Thickness of each air passage	1 in.
Length of total heat exchanger	20 in.
Volume of total heat exchanger	960 in ³ .
% Of room occupied	2.1%

Chapter 4: CAD Modelling

SOLIDWORKS is used to model the experimental model. One of the most popular software solutions for engineers is SOLIDWORKS, a solid modelling computer-aided design and computer-aided engineering package. The programme is first used for project management, planning, visual ideation, modelling, feasibility evaluation, prototyping, and feasibility assessment. After that, the programme is used to design and create mechanical, electrical, and software components. Finally, the programme may be used to manage devices, analytics, data automation, and cloud services.

Mechanical, electrical, and electronics professionals utilise the SOLIDWORKS software solutions to create an integrated design. The suite of applications is designed to keep all engineers in the loop and ready to respond quickly to design modifications or requests. We used SOLIDWORKS 2020.

4.1 Heat Exchanger Unit

The heat exchanger must be designed in accordance with the design standards outlined above.

It contains the following:

- Top Header
- Tubes
- Shell
- Bottom Header

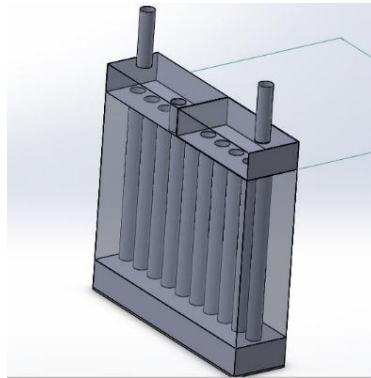


Figure 11: Single Exchanger Unit

The modelling of all pieces is covered in the sections that follow.

4.1.1 Top Header

The top header is divided into two parts, one for the inflow and one for the outflow. The water from the pump enters the inlet portion, which then distributes it to the tubes. The water is subsequently collected in the header's outflow part and delivered to the storage tank.

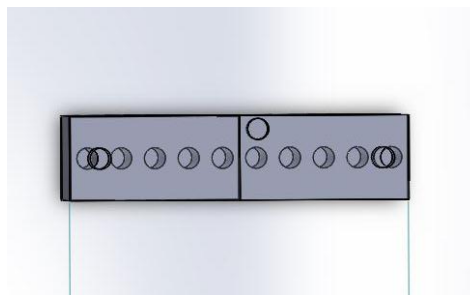


Figure 12: Top Header

4.1.2 Tubes

There are ten tubes in each of the unit. The tubes are connected with the inlet section of top header by which the water flows to the bottom header. These tubes are used to transfer heat to PCM in the shell.



Figure 13: A tube

4.1.3 Shell

PCM is filled into this shell by the hole at the top header. PCM contained in the shell is charged and discharged through water. PCM heats up the room when room temperature is lower than PCMs’.

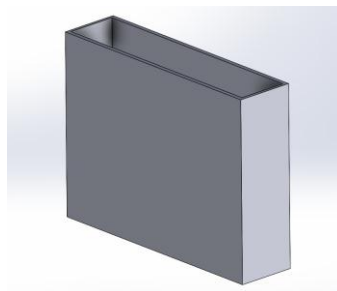


Figure 14: Shell

4.1.4 Main Header

Main header distributes water to seven units of the heat exchanger. This water flows with the help of the pump. Two main headers are attached to seven units for inlet and outlet of water through them from and to storage tank respectively.

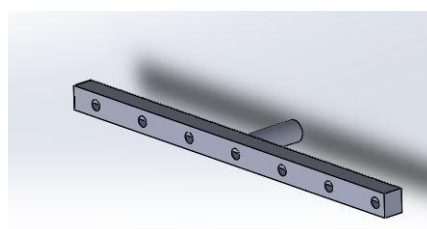


Figure 15: Bottom Header

4.2 Heat Exchanger Assembly

First three components are assembled and attached to a mounting frame. Two extended inlet and outlet pipes are connected to inlet and outlet section of top header.

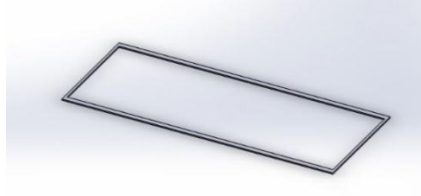


Figure 16: Mounting Frame

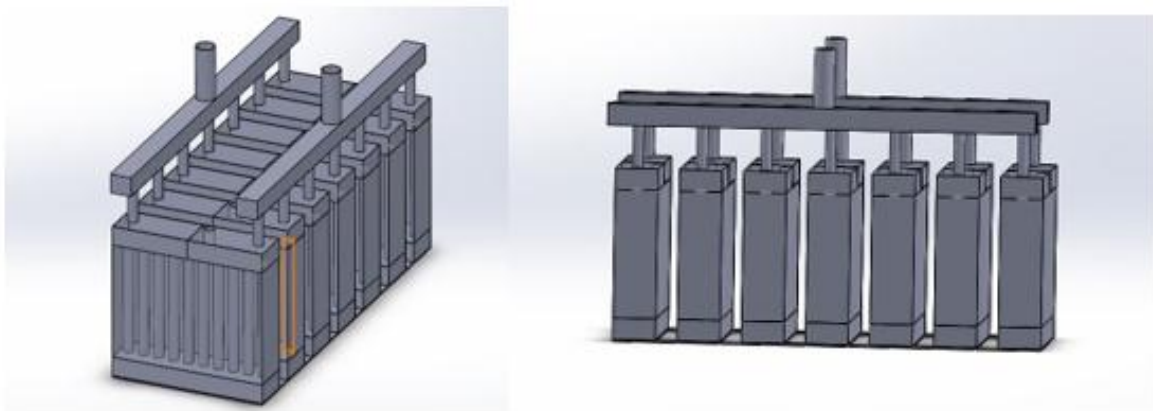


Figure 17: Heat Exchanger

Chapter 5: Fabrication and Component Procurement

In the light of the design and concept presented in the preceding sections, following components are required for the desired integrated system:

1. PCM shell and tube type heat exchanger
2. Control Room for experimentation
3. Pump
4. Fan
5. Styrofoam sheets
6. Plastic wrapping sheet
7. Clamps
8. K-type thermocouple
9. Arduino microcontroller
10. Flexible plastic pipes
11. Water storage tank

5.1 Procurements

A 25W pump was installed to circulate warm water throughout the heat exchanger. A ten-inch diameter fan was procured to add forced convection and consequently enhance the heat transfer mechanism. The power rating of the fan was 10W. Pump and Fan is the only load in the system and is of mere 35W. Six Styrofoam sheets were procured and were wrapped with plastic sheets on six faces of the experimental room. Flexible water pipes were attached using clamps to avoid leakage of water during water circulation. A k-type thermocouple was used to sample the room temperature during the experimentation. The sensor has accuracy of 0.1 °C with options of variable sampling time. An Arduino controller was configured to read and store data from the temperature sensor. A water storage tank was used to store and provide a continuous water circulation basis for the system

5.2 Fabrication of Single Heat Exchanger Unit

Various conventional manufacturing processing including shaping, drilling, welding etc. are involved in the manufacturing of the heat exchanger. The selected material was stainless steel. Better materials like copper and aluminium were rejected due to high material costs while cheap material like iron was rejected due its susceptibility to corrode. Therefore, an economical and equally reliable material stainless steel was selected.

The components of the designed heat exchangers are given in the list below:

1. Shell
2. Inlet Header
3. Outlet Header
4. Collector Header
5. Divider Plate
6. Water Inlet Pipes
7. Water Outlet Pipes
8. PCM Inlet Pipes
9. Main Inlet and Outlet Headers

Stainless steel sheets were cut and shaped in a U-bend to have minimum welding in the fabrication of the shell of heat exchanger. The remaining open sides of the U-bend were welded with steel plates. Argon welding was used instead of electrode welding to ensure a leakage free system. The dimensions of the shell thus fabricated were 6 x 8 x 2 inches.

Next square cross section pipes were cut to serve the purpose of headers. Inlet and outlet header had the dimensions of 4 x 2 x 1 inches. Their open sides were welded with steel plates to seal the headers. The plate in between the inlet and outlet header serves the purpose of keeping the inlet and outlet water separate from each other. A collector header that receives water from inlet pipe and directs it towards outlet pipes was fabricated using a square pipe. The dimensions of the collector pipe were 8 x 2 x 1 inches. Square pipes of 0.5 inches diameter and 6 inch in length were cut and welded up and down inside the holes drilled in the inlet, outlet and collector header. In a nutshell, each heat exchanger unit consists of one inlet, outlet and collector header along with a shell and ten circular tubes for water circulation. The fabricated heat exchanger unit is shown in Figure 18.



Figure 18: Single Exchanger Unit without Sheet Covering

5.3 Assembly of Fabricated Heat Exchanger Units

There was a requirement of seven heat exchanger units which had to be interconnected in parallel. All interconnected units would have a single inlet header that distributes water in the inlet pipes of all exchanger units and collects this water in a single main outlet header. Interconnection eliminates the need to connect inlet and outlet pipes at each unit, rather only two pipes with a pump installed in the reservoir would serve the purpose of circulation of water through the tubes to transfer heat to PCM. Main inlet and outlet header were made from square pipes cut to a dimension of 18 x 1 x 2 inches. Holes were drilled to weld them in the inlet and outlet pipes of all exchanger units.

The resulting assembly is shown in Figure 19



Figure 19: Top and Front View of Assembly

5.4 Fabrication of Control Room

The system was designed for specified volume of air i.e., 0.7 cubic meter. The dimensions of the room are 3 feet by 3 feet by 3 feet. Since the purpose of the room is to provide air space and keep it packed inside the room. The material did not really matter. Moreover, it was supposed to be insulated with Styrofoam sheets and wrapped with plastic sheet. Therefore, thin sheet of galvanized iron material was used to fabricate this control room. The room had buckles to lock it up and handles at the sides to facilitate the transportation. The fabricated room along with insulation on it is shown in Figure 20



Figure 20: Control Room

Chapter 6: CFD Validation

Ansys is a software explicitly developed for engineering simulations. This software offers various modules for simulating physics of various natures. Ansys Fluent is a module of Ansys, which is an extremely useful tool for simulating fluid and energy problems.

Ansys Fluent was used to simulate the temperature difference caused by PCM heat exchanger in the room. Following section presents and debates on the results and setups of PCM heat exchanger simulations in two dimensions and three dimensions.

6.1 Two-Dimensional Simulation

To setup a two-dimensional simulation, a geometry representing a plane of the three-dimensional geometry has to be modelled in a modelling software. The software used in this case was the design modular of Ansys. This section discusses in detail the ideology and methodology required for simulating the PCM heat exchanger in two-dimensions. Starting from geometry; creation of mesh, defining named selections for applying boundary conditions, application of boundary conditions, application of Multiphysics tool, patching, calculating and then eventually getting the results.

6.1.1 Two-Dimensional Domain Creation

To represent this model on two-dimensions, we need to create a rectangular domain. The rectangular sketch is converted into a surface. This rectangular surface would be modelled as the air in the room. Now the heat exchanger cross section as seen from the top view was sketched. This sketch was also converted into a surface. So, two-dimensional model consisted of two surfaces in total as shown in Figure 21.

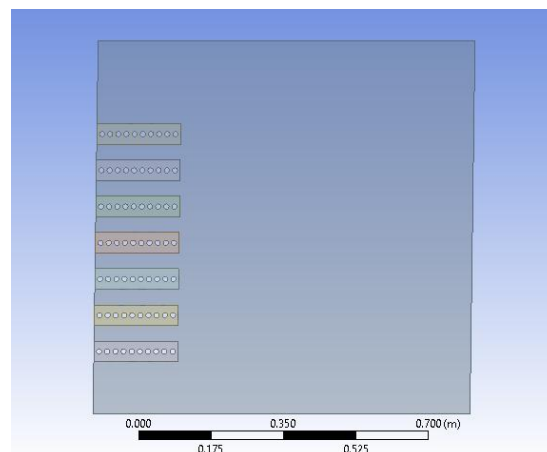


Figure 21: 2d geometry

6.1.2 Meshing

After the two-dimensional geometry creation, next task was to create nodes and elements on this geometry called meshing of the geometry. The solver uses these nodes for calculating the desired parameters. The outer surface representing air in the room was given a mesh size of 0.01 m. The heat exchanger surface was face meshed to an element size of 0.001 m. One hundred inflation layers were also added around the pipes of heat exchanger. The resulted meshed domain is shown in Figure 22.

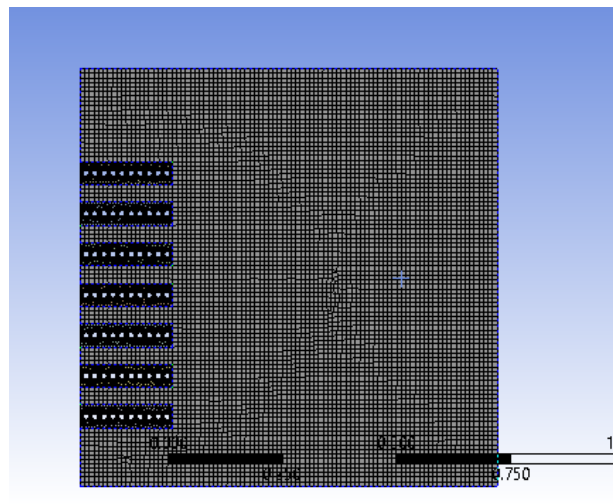


Figure 22: Structural Mesh

6.1.3 Boundary Conditions and Initialization

In meshing tool of Ansys, named selections were created at the locations where boundary conditions were to be applied. The boundary conditions include the adiabatic boundary at the walls and interface creation between heat exchanger walls and the room. The rest surfaces were initialized using the patch tool of Fluent. The heat exchanger was patched with a temperature of 46 °C while the room was initialized with a temperature of 30°C. The volume fraction of PCM was set to 1 in the heat exchanger and the rest of the room was automatically initialized with air.

6.1.4 Models Used

In Fluent, Multiphysics, energy, and solidification/melting modal was selecting to simulate the physics of this simulation. Multiphysics module allows more than one phase to interact. Heat transfer process in the room was modelled through energy modal while PCM material was manually added by checking the solidification/ melting module ON.

6.1.5 Calculation Activities

Since the PCM has lower thermal conductivity, the time step size does not need to be small. The time step size chosen was 10 seconds and iteration per step were reduced to 10. Number of time steps set were 1200 making a real simulation time of around three hours. SIMPLE scheme solver was used, and the frames were saved after every 5 iterations. The solution data export file was also set to calculate volume fraction of PCM. The solver was started to simulate the conditions, geometry and physics prescribed above.

6.1.6 Contour Plots and Results

CFD Tool-Post was used to analyze the results of the simulation. A plane was created to see the contour plot of temperatures during the three-hour simulation. As the solver was saving files during the simulation; the contour plot at each time step is available and could be merged together to observe a video of the simulation. The results showed a temperature increase of 12°C over a real time of three hours.

At the beginning of the simulation the contour plot showed the room air to be at a temperature of 30°C while the heat exchanger is at 46 °C and had started to transfer heat into the room. This contour plot is shown in Figure 23.

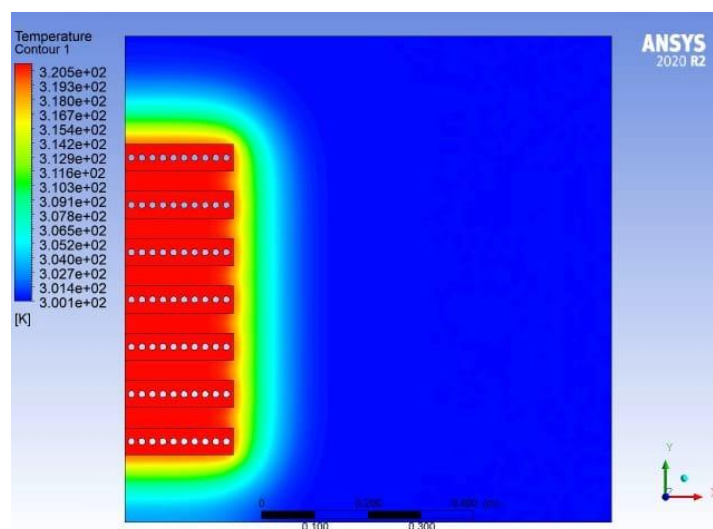


Figure 23: Initial Contour Plot of Temperature

At the end of the simulation, the temperature contour plot was seen to show a temperature difference of 12°C at the end furthest away from the heat exchanger. This contour plot is shown in the Figure 24.

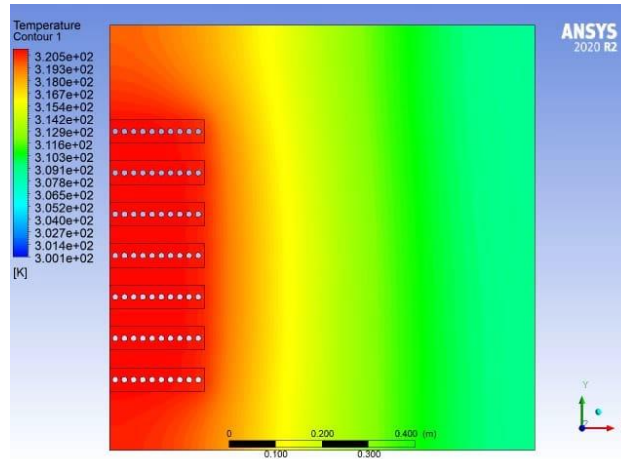


Figure 24: Final Temperature Contour Plot

The initial conditions and the final results are tabulated in Table 10

Table 10: Two-dimensional Simulation Results

Time (s)	Temperature at Further End of Room (°C)
0	30°C
10800 s	42°C

6.2 Three-Dimensional Simulation

Three-dimensional simulation is rather tedious to handle as compared to two-dimensional simulation. To reduce the computational cost of three-dimensional simulation. The geometry was scaled down. Therefore, instead of using seven interconnected units; a single unit could do the work. The air space was consequently reduced in same proportion to 0.1 cubic meter. The following section encompasses the detail of three-dimensional simulation.

6.2.1 Geometry Creation

For solving fluid problem in three-dimensions, fluid path, in addition to the geometrical structure had to be modeled. As said above, only one exchanger unit had to be modelled. This geometry mainly consisted of two domains: the water domain inside headers and pipes and PCM domain in the shell.

The three-dimensional representation of one unit of heat exchanger is shown in **Error! Reference source not found.**

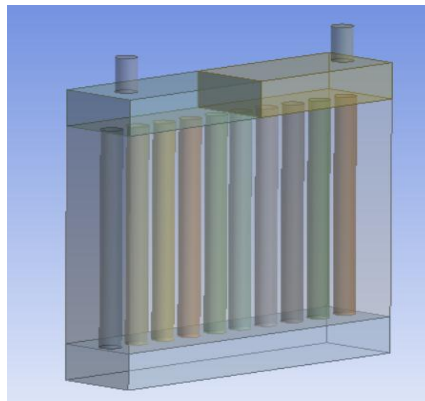


Figure 25: Three-Dimensional Simulation Geometry Representation

To model the air space of the room, an enclosure had to be created using enclosure command of design modular. The coordinates had to be carefully selected to properly place the heat exchanger inside the room. After the creation of room, it had to be Boolean out from the space that is covered by heat exchanger. This would create a perfect setup of real time experiment in which there is a room which is insulated from outside and is placed with a heat exchanger near one wall of the room.

The complete CAD model of the three-dimensional representation of the actual experiment is shown in Figure 26

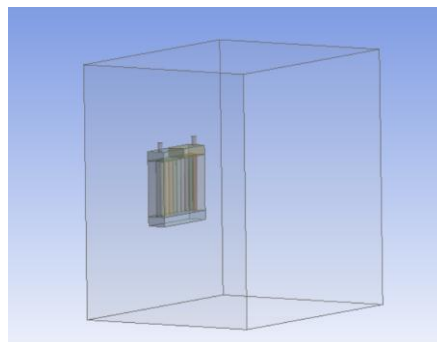


Figure 26: Overall Three-Dimensional Representation

6.2.2 Meshing

Due to large geometry and limitation of computational power, a simple mesh was generated with an element size of 0.01m. The nodes and elements created were 236445 and 777301 respectively. The heat exchanger model was further fined through edge sizing and face meshing.

The meshed geometry is shown in Figure 27.

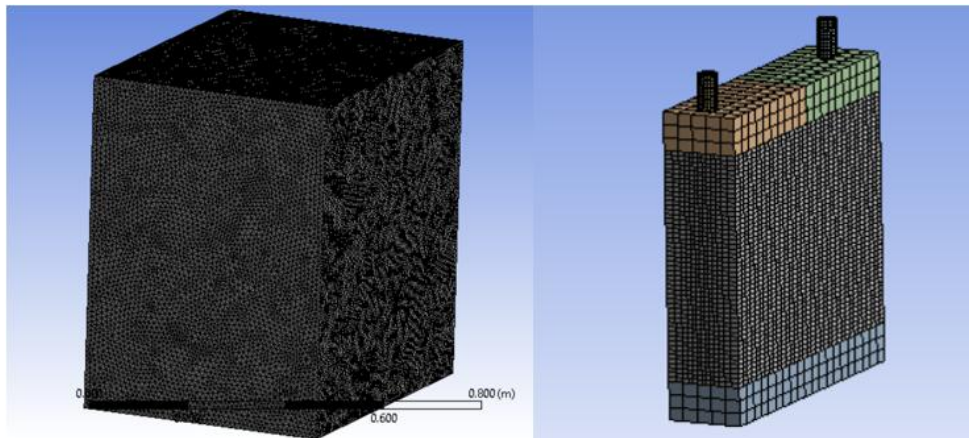


Figure 27: Three-Dimensional Mesh

6.2.3 Boundary Conditions and Initialization

To apply boundary conditions, named selections were created in the mesh tool. Walls, interiors, and interfaces were defined to set boundary conditions in Fluent later. The enclosure domain is to be patched as air at a temperature of 30°C while shell of the heat exchanger is to be patched with PCM volume fraction of 1 at a temperature of 46°C. The headers and pipes were initialized with water volume fraction of 1 at a temperature of 48°C. The left wall of the room was set at atmospheric pressure while the right side was set to a pressure of 101323.87 Pa to simulate forced convection by the movement of air by 1.5 meters per second due to this pressure difference.

6.2.4 Models

In Fluent, Multiphysics, energy, and solidification\ melting modal was selecting to simulate the physics of this simulation. Multiphysics module allows more than one phase to interact. Heat transfer process in the room was modelled through energy modal while PCM material was manually added by checking the solidification\ melting module ON. In Multiphysics, three phases air, water, and PCM were added. The surface tension between water and air was set to 0.072 N/m.

6.2.5 Calculation Activities

The time step size chosen was 0.1 seconds at the beginning to avoid divergence. It was increased gradually up till 10 seconds and iteration per step were reduced to 10. Number of

time steps set were 3000 making a real simulation time of around two hours. SIMPLE scheme solver was used and the frames were saved after every 5 iterations.

The solution data export file was also set to calculate volume fraction of PCM. The solver was started to simulate the conditions, geometry and physics prescribed above.

6.2.6 Contour Plots and Results

CFD Tool-Post was used to analyze the results of the simulation. A volume render was created to see the plot of temperatures in the three-dimensional space during the three-hour simulation. As the solver was saving files during the simulation; the volume render at each time step was available and could be merged together to observe a video of the simulation. The results showed a temperature increase 15°C of over a real time of two hours.

At the beginning of the simulation the volume render showed the room air to be at a temperature of 30°C while the PCM in heat exchanger was at 46°C as shown in Figure 28.

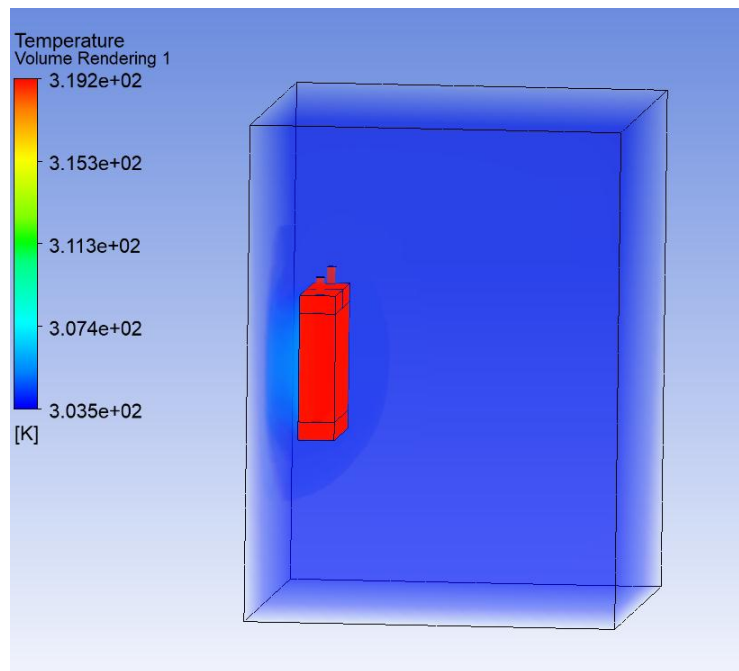


Figure 28: Volume Render at Start of the Simulation

At the end of the simulation, the temperature volume render was seen to show a temperature difference of 15°C at the end furthest away from the heat exchanger as shown in Figure 30.

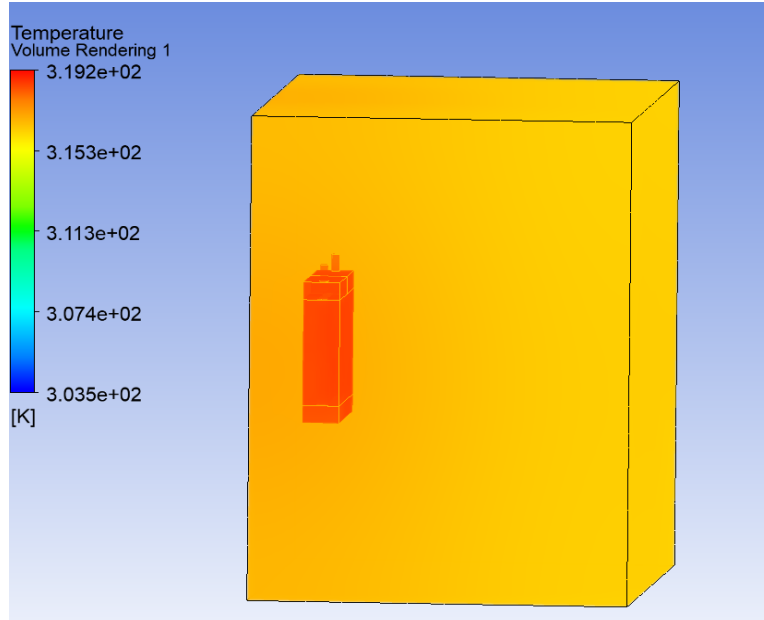


Figure 29: Volume Render at the End of Simulation

The results of this simulation are tabulated below:

Table 11: Results of Three-Dimensional Simulation

Time Step (s)	Temperature at Further End of Room (°C)
0	30
7200	45

Chapter 7: Experimentation

A suitable space was selected to conduct the experiment. Necessary precautions were taken, and safety was kept as highest responsibility. The lab atmospheric conditions were kept in mind and the experimentation was set to begin. This chapter contains the experimental setup along with the details and results comprising charging and discharging of PCM.

7.1 Actual Experiment

The experiment was carried out in order to put the system to the test in the actual world. The strategy was to integrate all the system's components so that any issues with the components could be resolved. By operating the system in a local setting, the goal was to achieve real results. The experimental results must be compared to the Ansys simulation results.

7.1.1 Installation

An experimental setup has been built to conduct the experiment. To begin, Styrofoam and plastic sheet are used to insulate the control room. Around the six sides of the control room, six sheets of Styrofoam have been affixed. Plastic sheet is placed over Styrofoam to insulate the space even further as shown in Figure 20.

The next step was to put the heat exchanger in a state where it could circulate water. A heat exchanger was installed within the control room for this reason. To ensure zero leakage, two thermal graded pipes have been tightly linked at the heat exchanger's intake and output. The other end of one of the pipes is attached with the pump and other one is placed into the water reservoir.

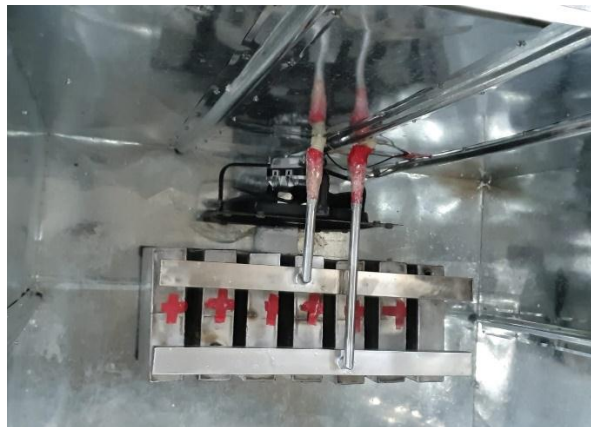


Figure 30: Experimental Setup

7.1.2 Auxiliary Components

A standard air cooler pump was utilized to circulate the water. The pump's rated power, flowrate and head were 25 W, 1000 litre/hour and 1.8 m respectively. A small DC fan was also put inside the control room with heat exchanger to ensure forced convection in the control room for high heat transfer.



Figure 31: Pump

A stove and steel bucket needed to heat the water. The stove is turned on hand water was heated inside bucket placed on it. The temperature of water was raised and maintained at 50 C. A digital sensor is being used to measure the temperature of water being heated by stove.



Figure 32: Thermostat

Vernier Surface Temperature Sensor was used to measure the temperature variations in control room. It has a range from -25 C° to 125 C° (-13 F° to 257 F°) with an accuracy of 0.5 C° . The maximum it can tolerate with damage is 150 C° .



Figure 33: Vernier Surface Temperature Sensor

Table 12 shows the specifications of vernier type temperature sensor.

Table 12: Vernier Surface Temperature Sensor Specifications

Temperature range	-25°C to 125°C (-13 to 275°F)
Maximum temperature that the sensor can tolerate without damage	150°C
13-bit resolution	0.04°C (-25 to 0°C) 0.02°C (0 to 40°C) 0.05°C (40 to 100°C) 0.13°C (100 to 125 °C) 0.08°C(-25 to 0°C)
12-bit resolution	0.08°C (-25 to 0°C) 0.03°C (0 to 40°C) 0.1°C (40 to 100°C) 0.25°C (100 to 125 °C)
10-bit resolution	0.32°C (-25 to 0°C) 0.12°C (0 to 40°C) 0.4°C (40 to 100°C) 1°C (100 to 125 °C)
Temperature sensor	20 KΩ NTC Thermistor
Accuracy	±0.2°C at 0°C, ±0.5°C at 100°C
Response time (time for 90% change in reading)	50 seconds (in still air) 20 seconds (in moving air)
Probe dimensions probe length (handle plus body)	15.5 cm

7.1.3 Arduino Setup

For the integration of the sensors Arduino setup was utilized. The Arduino connection was made with the breadboard using jumper wires while code was loaded in the laptop using the installed Arduino IDE.



Figure 34: Arduino Setup

Wiring procedure was aided from the vernier user manuals. Using the instructions provided by Vernier sketches, the Protoboard adapter was connected to the breadboard. It included six labelled pins and were connected as described.

- Wiring a Single Digital Protoboard Adapter: DIO0 (Vernier BTM pin 1) to Arduino pin 2 (function depends on sensor)
- DIO1 (Vernier BTM pin 2) to Arduino pin 3 (function depends on sensor)
- DIO2 (Vernier BTM pin 3) to Arduino pin 4 (function depends on sensor)
- 5V (Vernier BTM pin 4) to Arduino pin 5V (power)
- GND (Vernier BTM pin 5) to Arduino pin GND (ground)
- DIO3 (Vernier BTM pin 6) to Arduino pin 5 (function depends on sensor)

Code for Vernier Surface Temperature Sensor is given below:

```
#include "VernierLib.h" //include Vernier functions in this sketch
VernierLib Vernier; //create an instance of the VernierLib library
float sensorReading; //create global variable to store sensor reading
void setup() {
  Serial.begin(9600); //setup communication to display
  Vernier.autoID(); //identify the sensor being used
}
void loop() {
  sensorReading = Vernier.readSensor(); //read one data value
  Serial.print(sensorReading); //print data value
  Serial.print(" "); //print a space
  Serial.println(Vernier.sensorUnits()); //print units and skip to next line
  delay(500); //wait half second
}
```

As the setup was completed, a steel bucket was filled with water and placed on the stove. The stove was turned on to heat the water. When the temperature of water reached to 50°C the pumped was turned on to circulate water in the heat exchanger. In this way PCM got charged and tend to change its state from solid to liquid with heat dissipation in control room. The charging process continued for 4 hours. The rate of heat transfer increased by forced convection using a fan placed beside the heat exchanger. As the charging process completed and PCM turned liquid. The stove was turned off alongside the pump. Then the PCM was allowed to discharge in the control room for 1.5 hours.

7.2 Cautions

There were some cautions that were to be kept in check and required full supervision. They were significant factors in the conduction of the experiment. The team was present to keep check during the running time of the setup.

7.2.1 Leakage

A main concern during experiment setup and conduct was to stop leakages from water pipes specifically at connections. As the heated water flow through pipes, there was a high risk of pipe damage consequently the leakage which have been monitored during the experiment.

7.2.2 Pump Tripping

A room air cooler pump was being used for water circulation. The maximum temperature of water which can be flowed was 35°C. On contrary, water circulated through pump was at 50°C due which it got tripped after some interval. As a solution pump removed for some time, as it got cooled it again inserted in heated water to continue process.

7.2.3 Water Temperature

The stove being used for water heat was manually controlled to maintain temperature according to requirement. For this process, stove is turned, water temperature was raised. As it exceeded the required value being measured by thermostat, stove is turned off. The temperature of water reached to required value, as it stated to decrease stove is turned on once again.

7.2.4 Sensor Reading

One of the important cautions was to monitor the temperature reading continuously. Sometimes sensor started to give illogical readings due to connection break or communication breakage which have been sorted out to get maximum accurate and precise values.

7.3 Results

The data collected from conduction of the experiment consisted in two phases, charging and discharging of PCM. Data was processed by Arduino as discussed in 7.1.3 Arduino Setup and, then formulated in MS Excel for data plots.

7.3.1 Charging

The PCM was charged for 2 hours. The room temperature at the start of experiment was 30°C which became 46°C. During this period the temperature of control room rises to almost 16°C. This is depicted in Figure 35.

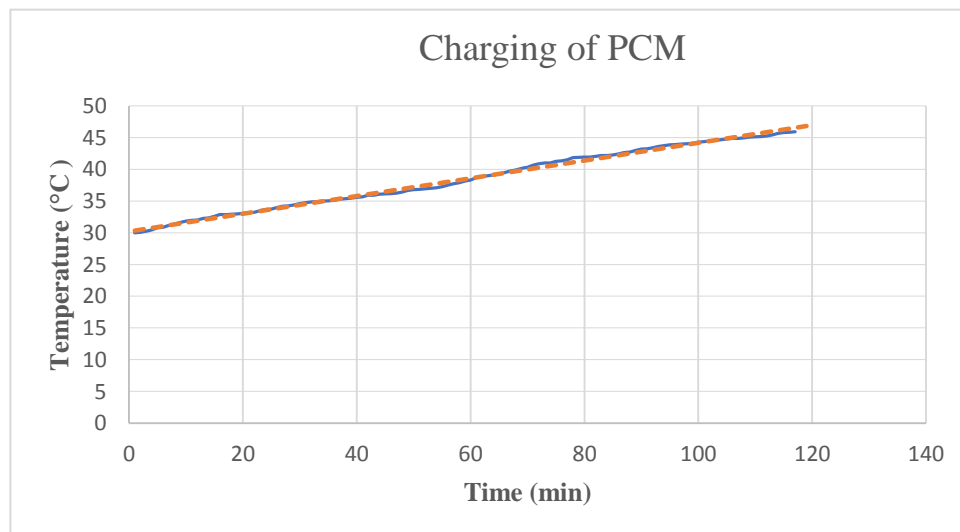


Figure 35: Charging Data Graph

7.3.2 Discharging

PCM discharged and energy is released from PCM to stabilize the temperature for some time. In the experiment, the temperature of control room was maintained and only decreased 30°C in two hours.

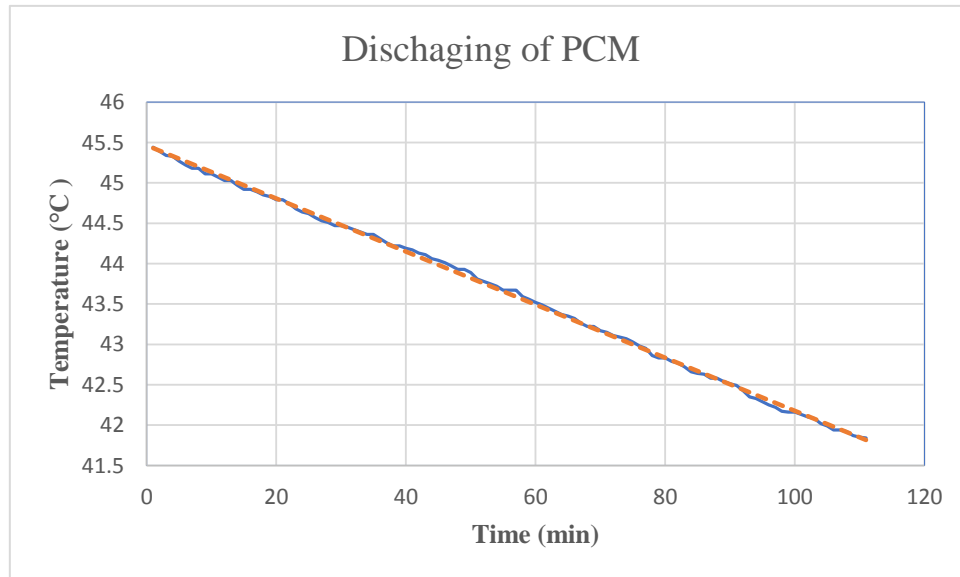


Figure 36: Discharging Data Graph

Chapter 8: Comparison of Results

The preceding sections covered the results of actual and multiple simulation results. This section would encompass the comparison of these results along with the debate on these results and the design calculations. Based on these discussions, recommendations for future researchers would be made in the subsequent sections.

Three different set of results were presented in the preceding sections that are listed below:

1. Actual Experimentation
2. Two-Dimensional Simulation
3. Three-Dimensional Simulation

All results were in close correspondence with each other.

A sophisticated comparison of two-dimensional and three-dimensional simulation with the actual experiment is given in Table 13.

Table 13: Results Comparison

Process	Time of Process	Temperature Rise	Relative Error with Actual Experiment
Actual Experiment	2 hours	16 °C	0 %
Two-Dimensional Simulation	2 hours	12 °C	25%
Three-Dimensional Simulation	2 hours	15 °C	6.25 %

Thus, actual experiment is in close correspondence with the simulations in particular with three-dimensional simulation. Two-dimensional simulation differs slightly from actual due to heat transfer, transfer coefficients, and gradients in planar surface rather than in integrated three-dimensional space.

Chapter 9: Discussion on Conventional Analysis Techniques

Among the possibilities for analyzing the performance of the full-scale PCM heat exchanger, the most appropriate technique for analyzing the performance of the full-scale PCM heat exchanger in this passive heating application is selected with justifications. These techniques are used for conventional applications and there are certain limitations in using these analytical techniques in the passive heating application. The reasons are discussed in Table 14.

Table 14: Adaptability of analysis techniques of PCM heat exchanger towards passive heating [87]

Technique	Adaptability to passive heating application
<p>Effectiveness-Number of Transfer Units (ϵ-NTU)</p> <p>Log Mean Temperature Difference (LMTD)</p>	<ul style="list-style-type: none"> • Because these methodologies are sizing based, using holistic thermal characteristics, the overall performance of the PCM heat exchanger is unknown, but the performance of a unit-volume is known, making applicability problematic. • Water, air, and the PCM make up the three-way heat exchanger in this application. Both approaches are suitable for sensible heat transmission but are ineffective in three-way thermal storage applications.

	<ul style="list-style-type: none"> • Because phase transition in a PCM involves a combination of convection and conduction, it's impossible to forecast the U-value for both melting and freezing, which are required in these approaches, theoretically. • Both models assume that the PCM's thermophysical properties are constant, even though they are non-homogeneous, non-linear, and inconsistent. The specific heat capacity of a PCM, for example, is non-linearly depending on the incoming heat flux. • Due to the transitory nature of this passive heating application, the accuracy of these steady state models is limited. The PCM would be treated as having a constant enthalpy in these methodologies, even though it varies non-proportionally with time.
<p style="text-align: center;">Conduction Transfer Functions (CTF)</p>	<ul style="list-style-type: none"> • For this application, the CTF approach is utilized to estimate mainly transient heat conduction in the PCM, not convection. As a result, modelling simply freezing and not melting is more appropriate. • Heat fluxes are computed using a time series technique based on surface temperatures. The presence of corrugations and fins on the pipes makes determining the total surface temperature impossible without the use of a numerical technique. • For this case, a finite element based multiple CTF value approach would be appropriate, but it would complicate things and provide limited precision.
<p style="text-align: center;">Dimensionless analysis to predict correlations</p>	<ul style="list-style-type: none"> • Basic correlations are generalized in dimensionless analysis to expand their usefulness in similar contexts. Such design equations have been created for certain geometries. • Because of the complexities of the geometry in this application, as well as the variable PCM behavior, developing such correlations would be exceedingly generic and imprecise. • Similarly, without numerical approaches, analytical correlations for PCM heat exchangers, particularly in 3D layouts, are non-existent and imprecise to calculate.
<p style="text-align: center;">Empirical correlations of useful parameters</p>	<ul style="list-style-type: none"> • Empirical relationships of relevant variables are formed based on experimental/numerical observations. It is the most widely used method for modelling PCM heat exchangers in innovative applications. The equations' validity, on the other hand, is limited to the specific application.

Chapter 10: Future Recommendations and Limitations

This section is comprised of future recommendations and limitation regarding the Phase Change Material Heat Exchanger Model

10.1 Future Recommendations

In the aristocratic goal of supplying clean and cost-free energy; solar PCM Systems clutch a bright future. Due to the low thermal conductivity of PCMs, solar PCM systems have always been confronted by the economics of their applicability. Therefore, immense care must be taken while designing such systems. In this spectrum, an encyclopedic review on novel design concepts of active and passive solar PCM systems was presented in this paper. The performance of the systems debated over in this review is adorable and economically applicable which has pronounced the spirit of research for further improvements and application of solar PCM Systems. Considering all matrices of performance, savings, and applicability; we conclude that active solar systems despite having some energy consuming components, provide better energy savings as compared to passive solar systems. The thermophysical properties of PCMs and technical design parameters influencing the performance of solar PCM systems were also enlightened. Moreover, the economics of solar PCM systems justifying the use of these systems were discussed in detail. Optimization of the key performance parameters has turned out to be extremely significant for the performance of these systems and has become a prime focus of researcher recently. In this regard, a comprehensive discussion on the optimization techniques was done in this paper. Numerical and simulation-based optimizations are the most powerful tools to serve this crucial purpose and are used in almost every research nowadays.

The debate of this paper established that solar PCM systems are now improved to an extent that they can be used practically. Even then, these systems have an immense ground to cover to compete electrical storage systems. In this regard, few future recommendations are listed below:

- Thermal conductivity of PCMs despite adapting several improvement techniques is still the main constraint that limits the efficiency of solar PCM systems and thus needs to be researched further.
- Research should be done to increase the density of PCMs, to decrease the volume of system and thus increasing energy storage.

- Configuration and geometry of tubes exchanging heat with PCM needs to be explored so that complete charging and discharging can be achieved withing short span of time.
- Optimization using algorithms such as genetic algorithm optimization has proved to be useful. Although these algorithms are complex but holds the potential of improving the performance of the system significantly. Therefore, development of similar algorithms is recommended for further improvements.
- Due to uncertain whether fluctuations, these systems should be tested under real conditions instead of simulated conditions for more accurate results.
- Focused research on prevention of energy loses should be done.
- Simulations should be done with real-time climatic data using user defined functions instead of constant radiation fluxes.

10.2 Limitations

This system has a few limitations when comprised with PCM. These restrictions have suppressed the benefits of the system resulting in limited use in industry. But advancements with time can take the system a long way ahead.

10.2.1 Phase Change Material

The use of a phase change materials (PCMs) is a very promising technology for thermal energy storage where it can absorb and release a large amount of latent heat during the phase transition process. The issues that have restricted the use of latent heat storage includes the following:

- Poor Thermal Conductivity
- High Density
- Heavy Weight

The study of the influence of thermal cycling on the properties of PCMs, such as melting temperature and latent heat, is important. It is found that the paraffin wax and fatty acids (e.g., lauric acid, myristic acid, palmitic acid, and stearic acid) have good thermal stability and can be used for solar thermal energy storage applications.

10.2.2 System Designed

The system designed in this paper has various restrictions that limits the use of PCM and the system industrially. The benefits can outweigh the limitations if overcome. Some of the restrictions of the system designed are listed below:

- Large Size
- Heavy Weight
- Mounting Difficulties
- Periodic Maintenance

Chapter 11: Conclusion

In the aristocratic goal of providing clean and free energy, passive PCM systems clutch a bright future as depicted from the literature review debated in the report. Moreover, the results of simulations and experimentation elevate the effectiveness of theses systems; but these systems have to cover a large ground before actually replacing the conventional fossil fuel systems. This report encompassed these limitations in detail and gave recommendations for improvement for future researchers. Furthermore, starting from the design basis and detailing up till the complete design and fabrication process; this paper gives a holistic elaboration of the novel design and fabricated model. The thickness of individual exchanger unit was only 2 inches to ensure proper melting of PCM. Further reduction in thickness will increase the effectiveness of the system. The actual experimental results differ from three-dimensional simulation by only 6.25% and two-dimensional simulation by 25%; the causes of which have been briefly discussed. The most promising parameters to improve these systems are the thermal conductivity of the system including the PCM itself, density of PCM, mounting feasibility in the room, and weight reduction.

REFERENCES

- [1] H. Xu, J. Y. Sze, A. Romagnoli, and X. Py, "Selection of Phase Change Material for Thermal Energy Storage in Solar Air Conditioning Systems," *Energy Procedia*, vol. 105, pp. 4281–4288, 2017, doi: 10.1016/j.egypro.2017.03.898.
- [2] Y. Kwon, M. Young, M. Hee, and J. Chul, "Energy & Buildings PCM cool roof systems for mitigating urban heat island - an experimental and numerical analysis," *Energy Build.*, vol. 205, p. 109537, 2019, doi: 10.1016/j.enbuild.2019.109537.
- [3] F. Souayfane, P. H. Biwole, F. Fardoun, and P. Achard, "Energy performance and economic analysis of a TIM-PCM wall under different climates," *Energy*, vol. 169, pp. 1274–1291, 2019, doi: 10.1016/j.energy.2018.12.116.
- [4] D. C. Iten, "Air-Multiple PCMs for the Free Cooling and Ventilation of Buildings Air-Multiple PCMs for the Free Cooling and Ventilation of Buildings," 2015.
- [5] T. Kousksou, P. Bruel, G. Cherreau, V. Leoussoff, and T. El Rhafiki, "PCM storage for solar DHW: From an unfulfilled promise to a real benefit," *Sol. Energy*, vol. 85, no. 9, pp. 2033–2040, 2011, doi: 10.1016/j.solener.2011.05.012.
- [6] J. Luo, D. Zou, Y. Wang, S. Wang, and L. Huang, "Battery thermal management systems (BTMs) based on phase change material (PCM): A comprehensive review," *Chem. Eng. J.*, vol. 430, no. P1, p. 132741, 2022, doi: 10.1016/j.cej.2021.132741.
- [7] E. Meng, R. Cai, Z. Sun, J. Yang, and J. Wang, "Experimental study of the passive and active performance of real-scale composite PCM room in winter," *Appl. Therm. Eng.*, vol. 185, no. December 2020, p. 116418, 2021, doi: 10.1016/j.applthermaleng.2020.116418.
- [8] I. Sarbu, *Advances in Building Services Engineering*, no. June 2017. 2021.
- [9] Z. Qiu, P. Li, Z. Wang, H. Zhao, and X. Zhao, *PCM and PCM Slurries and Their Application in Solar Systems*. 2019.
- [10] Y. Hu, P. K. Heiselberg, H. Johra, and R. Guo, "Experimental and numerical study of a PCM solar air heat exchanger and its ventilation preheating effectiveness," *Renew. Energy*, vol. 145, pp. 106–115, 2020, doi: 10.1016/j.renene.2019.05.115.
- [11] J. Zhao, Y. Ji, Y. Yuan, Z. Zhang, and J. Lu, "Seven operation modes and simulation models of solar heating system with PCM storage tank," *Energies*, vol. 10, no. 12, 2017, doi: 10.3390/en10122128.
- [12] A. Jamar, Z. A. A. Majid, W. H. Azmi, M. Norhafana, and A. A. Razak, "A review of water heating system for solar energy applications," *Int. Commun. Heat Mass Transf.*, vol. 76, pp. 178–187, 2016, doi: 10.1016/j.icheatmasstransfer.2016.05.028.
- [13] E. B. S. Mettawee and G. M. R. Assassa, "Experimental study of a compact PCM solar collector," *Energy*, vol. 31, no. 14, pp. 2958–2968, 2006, doi: 10.1016/j.energy.2005.11.019.
- [14] S. Yu, S. G. Jeong, O. Chung, and S. Kim, "Bio-based PCM/carbon nanomaterials composites with enhanced thermal conductivity," *Sol. Energy Mater. Sol. Cells*, vol. 120, no. PART B, pp. 549–554, 2014, doi: 10.1016/j.solmat.2013.09.037.

- [15] M. Kenisarin, K. Mahkamov, F. Kahwash, and I. Makhkamova, "Enhancing thermal conductivity of paraffin wax 53–57 °C using expanded graphite," *Sol. Energy Mater. Sol. Cells*, vol. 200, no. July 2017, p. 110026, 2019, doi: 10.1016/j.solmat.2019.110026.
- [16] D. H. Choi, J. Lee, H. Hong, and Y. T. Kang, "Thermal conductivity and heat transfer performance enhancement of phase change materials (PCM) containing carbon additives for heat storage application," *Int. J. Refrig.*, vol. 42, pp. 112–120, 2014, doi: 10.1016/j.ijrefrig.2014.02.004.
- [17] A. R. Mazhar, A. Shukla, and S. Liu, "International Journal of Thermal Sciences Numerical analysis of rectangular fins in a PCM for low-grade heat harnessing," *Int. J. Therm. Sci.*, vol. 152, p. 106306, 2020, doi: 10.1016/j.ijthermalsci.2020.106306.
- [18] M. Mumtaz, A. Khan, N. I. Ibrahim, I. M. Mahbubul, R. Saidur, and F. A. Al-sulaiman, "Evaluation of solar collector designs with integrated latent heat thermal energy storage : A review," vol. 166, no. March 2017, pp. 334–350, 2018, doi: 10.1016/j.solener.2018.03.014.
- [19] M. E. Zayed *et al.*, "Solar Energy Materials and Solar Cells Applications of cascaded phase change materials in solar water collector storage tanks : A review," *Sol. Energy Mater. Sol. Cells*, vol. 199, no. April, pp. 24–49, 2019, doi: 10.1016/j.solmat.2019.04.018.
- [20] R. M. Muthusivagami, R. Velraj, and R. Sethumadhavan, "Solar cookers with and without thermal storage — A review," vol. 14, pp. 691–701, 2010, doi: 10.1016/j.rser.2008.08.018.
- [21] S. M. Shalaby, M. A. Bek, and A. A. El-sebaili, "Solar dryers with PCM as energy storage medium : A review," *Renew. Sustain. Energy Rev.*, vol. 33, pp. 110–116, 2014, doi: 10.1016/j.rser.2014.01.073.
- [22] R. Chaturvedi, A. Islam, and K. Sharma, "Materials Today : Proceedings A review on the applications of PCM in thermal storage of solar energy," *Mater. Today Proc.*, vol. 43, pp. 293–297, 2021, doi: 10.1016/j.matpr.2020.11.665.
- [23] A. A. M. Omara and H. A. Mohammed, *Phase change materials (PCMs) for improving solar still productivity : a review*, vol. 139, no. 3. Springer International Publishing, 2020.
- [24] F. S. Javadi, H. S. C. Metselaar, and P. Ganesan, "Performance improvement of solar thermal systems integrated with phase change materials (PCM), a review," *Sol. Energy*, vol. 206, no. April, pp. 330–352, 2020, doi: 10.1016/j.solener.2020.05.106.
- [25] M. Arıcı, F. Bilgin, S. Nižetić, and H. Karabay, "PCM integrated to external building walls: An optimization study on maximum activation of latent heat," *Appl. Therm. Eng.*, vol. 165, p. 114560, 2020, doi: 10.1016/j.applthermaleng.2019.114560.
- [26] E. B. S. Mettawee and G. M. R. Assassa, "Thermal conductivity enhancement in a latent heat storage system," *Sol. Energy*, vol. 81, no. 7, pp. 839–845, 2007, doi: 10.1016/j.solener.2006.11.009.
- [27] P. Wang, H. Yao, Z. Lan, Z. Peng, Y. Huang, and Y. Ding, "Numerical investigation of PCM melting process in sleeve tube with internal fins," *Energy Convers. Manag.*, vol. 110, pp. 428–435, 2016, doi: 10.1016/j.enconman.2015.12.042.

- [28] A. Baniassadi, B. Sajadi, M. Amidpour, and N. Noori, "Economic optimization of PCM and insulation layer thickness in residential buildings," *Sustain. Energy Technol. Assessments*, vol. 14, pp. 92–99, 2016, doi: 10.1016/j.seta.2016.01.008.
- [29] K. Chopra, V. V. Tyagi, A. K. Pandey, R. K. Sharma, and A. Sari, "PCM integrated glass in glass tube solar collector for low and medium temperature applications: Thermodynamic & techno-economic approach," *Energy*, vol. 198, p. 117238, 2020, doi: 10.1016/j.energy.2020.117238.
- [30] K. Velmurugan, S. Kumarasamy, T. Wongwuttanasatian, and V. Seithtanabutara, "Review of PCM types and suggestions for an applicable cascaded PCM for passive PV module cooling under tropical climate conditions," *J. Clean. Prod.*, vol. 293, p. 126065, 2021, doi: 10.1016/j.jclepro.2021.126065.
- [31] H. Shamsi, M. Boroushaki, and H. Geraei, "Performance evaluation and optimization of encapsulated cascade PCM thermal storage," *J. Energy Storage*, vol. 11, pp. 64–75, 2017, doi: 10.1016/j.est.2017.02.003.
- [32] X. Jia, X. Zhai, and X. Cheng, "Thermal performance analysis and optimization of a spherical PCM capsule with pin-fins for cold storage," *Appl. Therm. Eng.*, vol. 148, no. November 2018, pp. 929–938, 2019, doi: 10.1016/j.applthermaleng.2018.11.105.
- [33] A. Allouhi *et al.*, "Optimization of melting and solidification processes of PCM: Application to integrated collector storage solar water heaters (ICSSWH)," *Sol. Energy*, vol. 171, no. July, pp. 562–570, 2018, doi: 10.1016/j.solener.2018.06.096.
- [34] R. Barzin, J. J. J. Chen, B. R. Young, and M. M. Farid, "Application of weather forecast in conjunction with price-based method for PCM solar passive buildings - An experimental study," *Appl. Energy*, vol. 163, pp. 9–18, 2016, doi: 10.1016/j.apenergy.2015.11.016.
- [35] S. Lu, J. Gao, H. Tong, S. Yin, X. Tang, and X. Jiang, "Model establishment and operation optimization of the casing PCM radiant floor heating system," *Energy*, vol. 193, p. 116814, 2020, doi: 10.1016/j.energy.2019.116814.
- [36] M. Mehrpooya, H. Hemmatabady, and M. H. Ahmadi, "Optimization of performance of Combined Solar Collector-Geothermal Heat Pump Systems to supply thermal load needed for heating greenhouses," *Energy Convers. Manag.*, vol. 97, pp. 382–392, 2015, doi: 10.1016/j.enconman.2015.03.073.
- [37] A. Rehman, S. Liu, and A. Shukla, "Numerical investigation of the heat transfer enhancement using corrugated pipes in a PCM for grey water harnessing," *Therm. Sci. Eng. Prog.*, vol. 23, no. March, p. 100909, 2021, doi: 10.1016/j.tsep.2021.100909.
- [38] M. E. Afshan, A. S. Selvakumar, R. Velraj, and R. Rajaraman, "Effect of aspect ratio and dispersed PCM balls on the charging performance of a latent heat thermal storage unit for solar thermal applications," *Renew. Energy*, vol. 148, pp. 876–888, 2020, doi: 10.1016/j.renene.2019.10.172.
- [39] X. Kong, L. Wang, H. Li, G. Yuan, and C. Yao, "Experimental study on a novel hybrid system of active composite PCM wall and solar thermal system for clean heating supply in winter," *Sol. Energy*, vol. 195, no. February 2019, pp. 259–270, 2020, doi: 10.1016/j.solener.2019.11.081.
- [40] K. Saa and N. Daouas, "Energy and cost efficiency of phase change materials

- integrated in building envelopes under Tunisia Mediterranean climate,” vol. 187, 2019, doi: 10.1016/j.energy.2019.115987.
- [41] N. Zhu, M. Wu, P. Hu, L. Xu, F. Lei, and S. Li, “Performance study on different location of double layers SSPCM wallboard in office building,” *Energy Build.*, vol. 158, pp. 23–31, 2018, doi: 10.1016/j.enbuild.2017.09.075.
- [42] X. Jin, M. A. Medina, and X. Zhang, “Numerical analysis for the optimal location of a thin PCM layer in frame walls,” *Appl. Therm. Eng.*, vol. 103, pp. 1057–1063, 2016, doi: 10.1016/j.applthermaleng.2016.04.056.
- [43] D. Heim and J. A. Clarke, “Numerical modelling and thermal simulation of PCM-gypsum composites with ESP-r,” *Energy Build.*, vol. 36, no. 8, pp. 795–805, 2004, doi: 10.1016/j.enbuild.2004.01.004.
- [44] M. Sovetova, S. A. Memon, and J. Kim, “Thermal performance and energy efficiency of building integrated with PCMs in hot desert climate region,” *Sol. Energy*, vol. 189, no. July, pp. 357–371, 2019, doi: 10.1016/j.solener.2019.07.067.
- [45] Y. Qu, D. Zhou, F. Xue, and L. Cui, “Multi-factor analysis on thermal comfort and energy saving potential for PCM-integrated buildings in summer,” *Energy Build.*, vol. 241, 2021, doi: 10.1016/j.enbuild.2021.110966.
- [46] M. Alam, H. Jamil, J. Sanjayan, and J. Wilson, “Energy saving potential of phase change materials in major Australian cities,” *Energy Build.*, vol. 78, pp. 192–201, 2014, doi: 10.1016/j.enbuild.2014.04.027.
- [47] H. Wang, W. Lu, Z. Wu, and G. Zhang, “Parametric analysis of applying PCM wallboards for energy saving in high-rise lightweight buildings in Shanghai,” *Renew. Energy*, vol. 145, pp. 52–64, 2020, doi: 10.1016/j.renene.2019.05.124.
- [48] J. Zhao, Y. Ji, Y. Yuan, Z. Zhang, and J. Lu, “Energy-saving analysis of solar heating system with PCM storage tank,” *Energies*, vol. 11, no. 1, 2018, doi: 10.3390/en11010237.
- [49] P. Devaux and M. M. Farid, “Benefits of PCM underfloor heating with PCM wallboards for space heating in winter,” *Appl. Energy*, vol. 191, pp. 593–602, 2017, doi: 10.1016/j.apenergy.2017.01.060.
- [50] F. Calise, F. L. Cappiello, M. Dentice, and M. Vicidomini, “Dynamic modelling and thermo-economic analysis of micro wind turbines and building integrated photovoltaic panels,” *Renew. Energy*, vol. 160, pp. 633–652, 2020, doi: 10.1016/j.renene.2020.06.075.
- [51] G. P. Panayiotou, S. A. Kalogirou, and S. A. Tassou, “Evaluation of the application of Phase Change Materials (PCM) on the envelope of a typical dwelling in the Mediterranean region,” *Renew. Energy*, vol. 97, pp. 24–32, 2016, doi: 10.1016/j.renene.2016.05.043.
- [52] X. Mi, R. Liu, H. Cui, S. A. Memon, F. Xing, and Y. Lo, “Energy and economic analysis of building integrated with PCM in different cities of China,” *Appl. Energy*, vol. 175, pp. 324–336, 2016, doi: 10.1016/j.apenergy.2016.05.032.
- [53] E. Solgi, S. Memarian, and G. Nemati Moud, “Financial viability of PCMs in countries with low energy cost: A case study of different climates in Iran,” *Energy Build.*, vol. 173, pp. 128–137, 2018, doi: 10.1016/j.enbuild.2018.05.028.

- [54] S. U. S. Climates, J. Kosny, N. Shukla, and A. Fallahi, “Cost Analysis of Simple Phase Change Material-Enhanced Building Envelopes in,” no. January, 2013.
- [55] F. Souayfane, F. Fardoun, and P. H. Biwole, “Phase change materials (PCM) for cooling applications in buildings: A review,” *Energy Build.*, vol. 129, pp. 396–431, 2016, doi: 10.1016/j.enbuild.2016.04.006.
- [56] B. Y. Yun, J. H. Park, S. Yang, S. Wi, and S. Kim, “Integrated analysis of the energy and economic efficiency of PCM as an indoor decoration element: Application to an apartment building,” *Sol. Energy*, vol. 196, no. May 2019, pp. 437–447, 2020, doi: 10.1016/j.solener.2019.12.006.
- [57] A. Figueiredo, R. Vicente, J. Lapa, C. Cardoso, F. Rodrigues, and J. Kämpf, “Indoor thermal comfort assessment using different constructive solutions incorporating PCM,” *Appl. Energy*, vol. 208, no. March, pp. 1208–1221, 2017, doi: 10.1016/j.apenergy.2017.09.032.
- [58] D. Haillot, E. Franquet, S. Gibout, and J. P. Bédécarrats, “Optimization of solar DHW system including PCM media,” *Appl. Energy*, vol. 109, pp. 470–475, 2013, doi: 10.1016/j.apenergy.2012.09.062.
- [59] S. M. Salih, J. M. Jalil, and S. E. Najim, “Experimental and numerical analysis of double-pass solar air heater utilizing multiple capsules PCM,” *Renew. Energy*, vol. 143, pp. 1053–1066, 2019, doi: 10.1016/j.renene.2019.05.050.
- [60] Q. Mao and M. Yang, “Study on heat transfer performance of a solar double-slope PCM glazed roof with different physical parameters,” *Energy Build.*, vol. 223, p. 110141, 2020, doi: 10.1016/j.enbuild.2020.110141.
- [61] L. Navarro, A. de Gracia, A. Castell, and L. F. Cabeza, “Experimental study of an active slab with PCM coupled to a solar air collector for heating purposes,” *Energy Build.*, vol. 128, pp. 12–21, 2016, doi: 10.1016/j.enbuild.2016.06.069.
- [62] J. C. Frutos Dordelly, M. El Mankibi, L. Roccamena, G. Remion, and J. Arce Landa, “Experimental analysis of a PCM integrated solar chimney under laboratory conditions,” *Sol. Energy*, vol. 188, no. February, pp. 1332–1348, 2019, doi: 10.1016/j.solener.2019.06.065.
- [63] W. Ke, J. Ji, L. Xu, B. Yu, X. Tian, and J. Wang, “Numerical study and experimental validation of a multi-functional dual-air-channel solar wall system with PCM,” *Energy*, vol. 227, p. 120434, 2021, doi: 10.1016/j.energy.2021.120434.
- [64] M. Esen, “Thermal performance of a solar-aided latent heat store used for space heating by heat pump,” *Sol. Energy*, vol. 69, no. 1, pp. 15–25, 2000, doi: 10.1016/S0038-092X(00)00015-3.
- [65] M. Saffari, A. de Gracia, S. Ushak, and L. F. Cabeza, “Passive cooling of buildings with phase change materials using whole-building energy simulation tools: A review,” *Renew. Sustain. Energy Rev.*, vol. 80, no. May 2016, pp. 1239–1255, 2017, doi: 10.1016/j.rser.2017.05.139.
- [66] V. V. Tyagi and D. Buddhi, “PCM thermal storage in buildings: A state of art,” *Renew. Sustain. Energy Rev.*, vol. 11, no. 6, pp. 1146–1166, 2007, doi: 10.1016/j.rser.2005.10.002.
- [67] C. Voelker, O. Kornadt, and M. Ostry, “Temperature reduction due to the application

- of phase change materials,” *Energy Build.*, vol. 40, no. 5, pp. 937–944, 2008, doi: 10.1016/j.enbuild.2007.07.008.
- [68] S. Jeong, S. Wi, S. Jin, J. Lee, and S. Kim, “Energy & Buildings An experimental study on applying organic PCMs to gypsum-cement board for improving thermal performance of buildings in different climates,” *Energy Build.*, vol. 190, pp. 183–194, 2019, doi: 10.1016/j.enbuild.2019.02.037.
- [69] N. Shukla, A. Fallahi, and J. Kosny, “Performance characterization of PCM impregnated gypsum board for building applications,” vol. 30, pp. 370–379, 2012, doi: 10.1016/j.egypro.2012.11.044.
- [70] Y. Shen *et al.*, “Experimental thermal study of a new PCM-concrete thermal storage,” *Constr. Build. Mater.*, vol. 293, p. 123540, 2021, doi: 10.1016/j.conbuildmat.2021.123540.
- [71] A. G. Entrop, H. J. H. Brouwers, and A. H. M. E. Reinders, “Experimental research on the use of micro-encapsulated Phase Change Materials to store solar energy in concrete floors and to save energy in Dutch houses,” *Sol. Energy*, vol. 85, no. 5, pp. 1007–1020, 2011, doi: 10.1016/j.solener.2011.02.017.
- [72] D. Cano, C. Funéz, L. Rodriguez, J. L. Valverde, and L. Sanchez-silva, “Experimental investigation of a thermal storage system using phase change materials,” *Appl. Therm. Eng.*, vol. 107, pp. 264–270, 2016, doi: 10.1016/j.applthermaleng.2016.06.169.
- [73] M. Mahdaoui *et al.*, “Building bricks with phase change material (PCM): Thermal performances,” *Constr. Build. Mater.*, vol. 269, p. 121315, 2021, doi: 10.1016/j.conbuildmat.2020.121315.
- [74] T. Muthuvelan, K. Panchabikesan, R. Munisamy, K. M. Nibhanupudi, and V. Ramalingam, “Advances in Building Energy Research Experimental investigation of free cooling using phase change material-filled air heat exchanger for energy efficiency in buildings,” *Adv. Build. Energy Res.*, vol. 12, no. 2, pp. 139–149, 2018, doi: 10.1080/17512549.2016.1248487.
- [75] S. Duan, L. Wang, Z. Zhao, and C. Zhang, “Experimental study on thermal performance of an integrated PCM Trombe wall,” *Renew. Energy*, vol. 163, pp. 1932–1941, 2021, doi: 10.1016/j.renene.2020.10.081.
- [76] S. Li, N. Zhu, P. Hu, F. Lei, and R. Deng, “Numerical study on thermal performance of PCM Trombe Wall,” *Energy Procedia*, vol. 158, pp. 2441–2447, 2019, doi: 10.1016/j.egypro.2019.01.317.
- [77] I. Structures, *PCM-Enhanced Building Components*. .
- [78] T. Silva, R. Vicente, F. Rodrigues, A. Samagaio, and C. Cardoso, “Development of a window shutter with phase change materials: Full scale outdoor experimental approach,” *Energy Build.*, vol. 88, pp. 110–121, 2015, doi: 10.1016/j.enbuild.2014.11.053.
- [79] A. L. S. Chan, “Energy and environmental performance of building facades integrated with phase change material in subtropical Hong Kong,” *Energy Build.*, vol. 43, no. 10, pp. 2947–2955, 2011, doi: 10.1016/j.enbuild.2011.07.021.
- [80] Y. Choi, M. Mae, and H. Bae, “Thermal performance improvement method for air-based solar heating systems,” *Sol. Energy*, vol. 186, no. April, pp. 277–290, 2019, doi:

- 10.1016/j.solener.2019.04.061.
- [81] S. Mousavi, B. Rismanchi, S. Brey, and L. Aye, “PCM embedded radiant chilled ceiling : A state-of-the-art review,” *Renew. Sustain. Energy Rev.*, vol. 151, no. September, p. 111601, 2021, doi: 10.1016/j.rser.2021.111601.
- [82] J. M. Gutherz and M. E. Schiler, “A Passive Solar Heating System for the Perimeter Zone of Office Buildings A Passive Solar Heating System for the Perimeter Zone of Office Buildings,” vol. 8312, no. June, 2016, doi: 10.1080/00908319108908967.
- [83] H. R. Abbasi and H. Pourrahmani, “Multi-objective optimization and exergoeconomic analysis of a continuous solar-driven system with PCM for power, cooling and freshwater production,” *Energy Convers. Manag.*, vol. 211, no. March, p. 112761, 2020, doi: 10.1016/j.enconman.2020.112761.
- [84] P. Lamberg and K. Sirén, “Approximate analytical model for solidification in a finite PCM storage with internal fins,” *Appl. Math. Model.*, vol. 27, no. 7, pp. 491–513, 2003, doi: 10.1016/S0307-904X(03)00080-5.
- [85] W. Xiao, X. Wang, and Y. Zhang, “Analytical optimization of interior PCM for energy storage in a lightweight passive solar room,” *Appl. Energy*, vol. 86, no. 10, pp. 2013–2018, 2009, doi: 10.1016/j.apenergy.2008.12.011.
- [86] O. Rauf, S. Wang, P. Yuan, and J. Tan, “An overview of energy status and development in Pakistan,” *Renew. Sustain. Energy Rev.*, vol. 48, no. January 2012, pp. 892–931, 2015, doi: 10.1016/j.rser.2015.04.012.
- [87] A. Rehman, Y. Zou, S. Liu, Y. Shen, and A. Shukla, “Development of a PCM-HE to harness waste greywater heat : A case study of a residential building,” *Appl. Energy*, vol. 307, no. October 2021, p. 118164, 2022, doi: 10.1016/j.apenergy.2021.118164.